Article

Synthesis and properties of carbaporphyrin and carbachlorin dimethyl esters derived from cyclopentanedialdehydes

Navneet Sahota, Gregory M. Ferrence, and Timothy D. Lash

J. Org. Chem., **Just Accepted Manuscript** • DOI: 10.1021/acs.joc.7b01831 • Publication Date (Web): 29 Aug 2017

Synthesis and properties of carbaporphyrin and carbachlorin dimethyl esters derived from cyclopentanedialdehydes

Navneet Sahota, Gregory M. Ferrence and Timothy D. Lash*

Department of Chemistry, Illinois State University, Normal, Illinois 61790-4160

Abstract

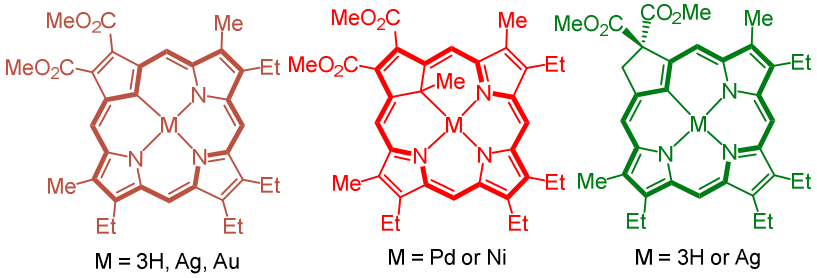

Norbornenes with two ester substituents were prepared by Diels-Alder cycloadditions of cyclopentadiene with dimethyl fumarate and dimethyl 1,1-ethylenedicarboxylate. Oxidation with potassium permanganate gave good yields of related diols that were oxidatively ring opened to afford cyclopentane dialdehydes. MacDonald-type "3 + 1" condensations with a tripyrrane, followed by oxidation with DDQ in refluxing toluene, gave carbaporphyrin or carbachlorin products in good yields. The macrocyclic products were highly diatropic and produced porphyrin-like UV-Vis spectra. The carbaporphyrin was converted into silver(III) and gold(III) organometallic derivatives. Reaction with methyl iodide in the presence of potassium carbonate gave mono- and dialkylation products, and treatment of the former with $Ni(OAc)_2$ or $Pd(OAc)_2$ afforded nickel(II) and palladium(II) complexes. The free base carbaporphyrin and carbachlorin, and the nickel and palladium complexes, were characterized by X-ray crystallography. The carbachlorin also reacted with silver(I) acetate to give a silver(III) derivative. Carbaporphyrins

and carbachlorins underwent deuterium exchange at the *meso*-positions with deuteriated TFA and this observation indicates that protonation is occurring at the bridging carbons. The new route to carbaporphyrins and carbachlorins has enabled detailed studies on the properties of these systems and provides the foundations for future investigations.

Introduction

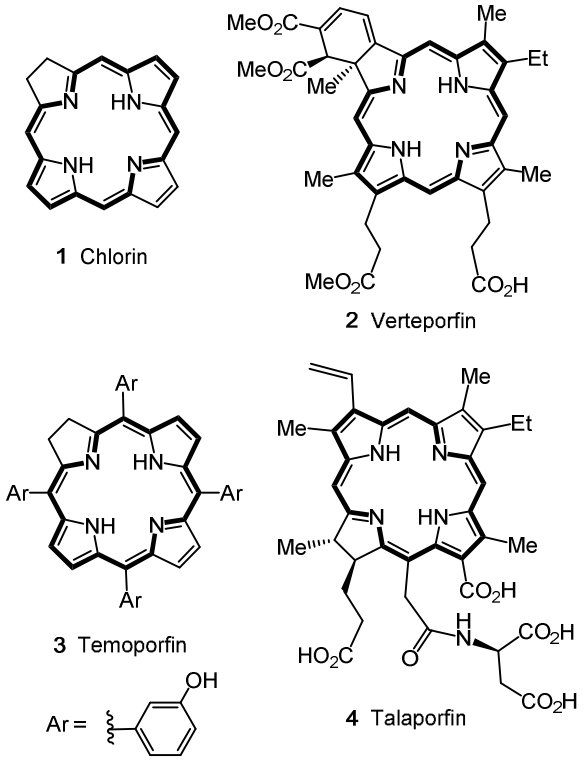

Chart 1. Chlorin and medicinally active derivatives

Chlorins **1** are 2,3-dihydroporphyrins that are widespread in nature.[1] In particular, many of the chlorophylls are magnesium chlorins and these play crucial roles in photosynthesis.[2] In addition, certain bacteria produce the iron(II) chlorin heme d,[3] while the marine echiuran worm *Bonellia viridis* produces a chlorin derivative called bonellin that is responsible for

masculinization of the larvae and also exhibits antitumor activity.[4] Chlorophyll-derived chlorins that possess antioxidant properties have been isolated from marine sponges, diatoms, tunicates and molusks.[5] Chlorins also have medicinal applications as photosensitizers in photodynamic therapy (PDT) (Chart 1). Verteporfin (Visudyne®, **2**) has been approved for the treatment of age-related macular degeneration[6] and has shown promise in atheroschlerotic plaque therapy.[7] Temoporfin (**3**) is being used for the PDT treatment of squamous cell carcinomas,[8] while talaporfin (**4**) has been approved for lung cancer.[9] Chlorins commonly have electronic absorptions above 650 nm and this feature is beneficial in PDT applications as light penetration in bodily tissues is more effective at longer wavelengths.[10,11] Unfortunately chlorin analogues have received very little attention,[12] although structures of this type could potentially be equally effective.

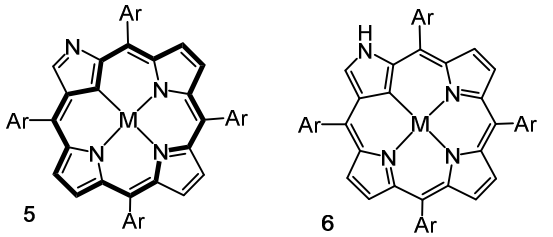

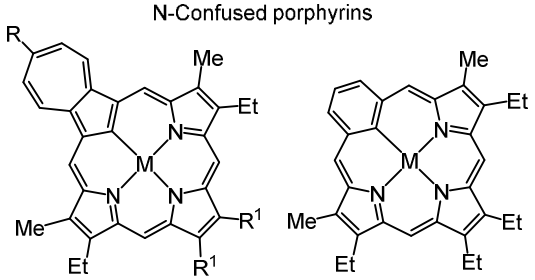

Chart 2. Carbaporphyrinoid systems

Investigations into carbaporphyrinoid systems continue to extend the structural diversity of porphyrin analogues.[13] Carbaporphyrinoids possess a porphyrin-like framework where one or more of the core nitrogen atoms have been replaced with carbons. Of these, N-Confused porphyrins **5a** (Chart 2) are the best studied and many examples of metalated derivatives for this system (e.g., **5b,c** and **6**) have been reported.[14] Structurally diverse carbaporphyrinoids have been synthesized, including azuliporphyrins **7a**[15] and benziporphyrins **8a**.[16] Macrocycles **7a** and **8a** generally act as dianionic ligands and a wide range of transition metal complexes have been reported (Chart 2).[17-19] True carbaporphyrins such as **9a**[20] and **10**[21] (Chart 3) contain cyclopentadiene subunits in place of one or more pyrrolic moiety and are commonly prepared as benzo-fused structures. Benzocarbaporphyrins can be prepared in excellent yields using the "3 + 1" variant on the MacDonald condensation.[22] However, only moderate yields were obtained in the synthesis of carbaporphyrins with unsubstituted cyclopentadiene subunits. Carbaporphyrins act as trianionic ligands and form silver(III), gold(III), rhodium(III) and iridium(III) complexes **9b-e**.[23,24] Reaction of carbaporphyrin **9a** with methyl iodide and potassium carbonate in refluxing acetone gave *N*-methylcarbaporphyrin **11a** as the major product together with *C*-methyl derivative **11b**.[25] Similarly **9a** reacted with ethyl iodide to afford **11c** (major) and **11d** (minor). *N*-Alkylcarbaporphyrins **11a** and **11c** could be metalated with palladium(II) acetate in refluxing acetonitrile to produce palladium(II) complexes **12a** and **12b**, respectively, where an unexpected alkyl group migration had also taken place.[25] Related metallocarbaporphyrins have been obtained indirectly by the ring contraction of metalated benziporphyrins.[26-28]

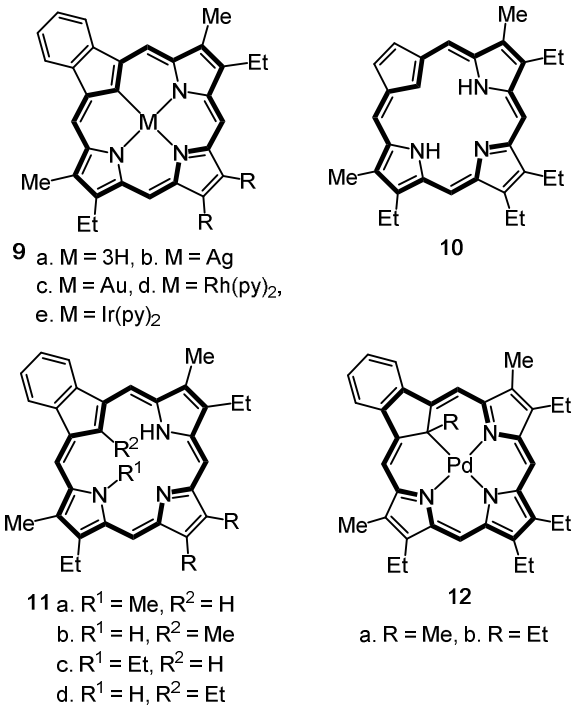

Chart 3. True carbaporphyrins and their metalated derivatives

Carbachlorins have also been prepared by the MacDonald-type "3 + 1" strategy, although much lower yields were obtained.[21,29] In an early study, bicyclic dialdehydes **13**, derived in two steps from the dimer of cyclopentadiene, were reacted with tripyrrane **14** in the presence of trifluoroacetic acid (TFA), and subsequent oxidation with DDQ in refluxing toluene afforded carbachlorins **15** in 11-15% yield (Scheme 1).[29] Attempts to oxidize **15a** or **15b** to the corresponding carbaporphyrins were unsuccessful even though most chlorins are readily converted to porphyrins under mild oxidative conditions. In a more recent investigation, ethoxymethylenecyclopentene carbaldehyde **16** was reacted with **14** under similar conditions and following oxidation with aqueous ferric chloride, carbachlorin **17** was isolated in 11-16% yield.[21] A dicarbachlorin was prepared in 5-7% yield from dicyclopentadienylmethane,[30] while a

thiacarbachlorin was obtained in 5% yield by reacting a carbatripyrrene with a thiophene dicarbinol.[31] Unlike **15a** and **15b**, carbachlorin **17** was easily dehydrogenated with DDQ to give carbaporphyrin **10**.[21] Reaction of **17** with silver(I) acetate afforded silver(III) complex **18**, while alkylation with methyl iodide afforded the *N*-methyl derivative **19**.[21] Treatment with palladium(II) acetate in acetonitrile led to a metalation-oxidation-alkyl group migration cascade to generate the palladium(II) complex **20**.[21] It is notable that the UV-vis spectra for **15a**, **15b** and **17** all gave moderately strong absorptions at 650-651 nm.[21,29]

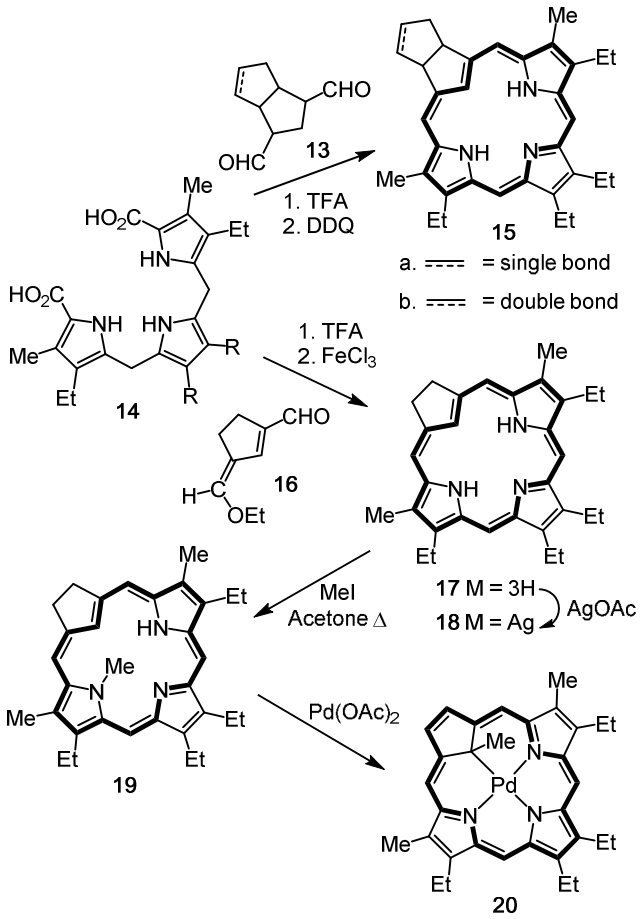

Scheme 1. Examples of earlier syntheses and metalations of carbaporphyrins.

Although carbachlorins possess potentially useful spectroscopic properties and display interesting chemical reactivity, further studies have been limited due to the mediocre yields obtained for previously reported syntheses. In this work, we set out to develop a superior methodology for preparing carbachlorins and carbaporphyrins without fused aromatic units. This work has resulted in the generation of new carbachlorins and carbaporphyrins and has enabled the formation and structural characterization of novel organometallic derivatives.[32]

Results and discussion

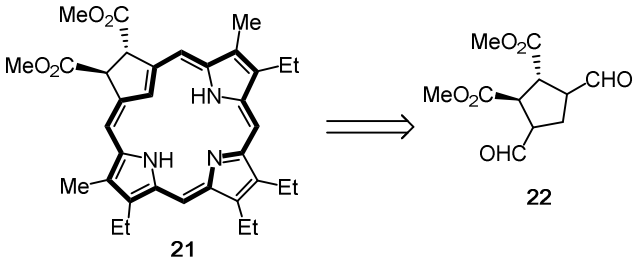

Scheme 2. Retrosynthetic analysis of carbachlorin **21**.

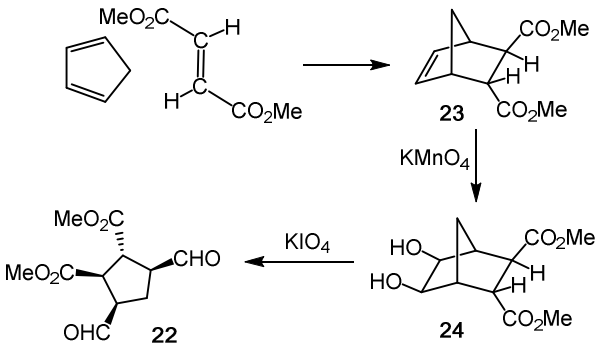

Scheme 3. Synthesis of a cyclopentane dialdehyde from dimethyl fumarate.

Benzocarbaporphyrins such as **9a** are robust compounds with intriguing reactivity.[20] However, although carbaporphyrin **10** is quite stable in solution, it appears to be far more prone

to degradation reactions. In the case of a related thiacarbaporphyrin, this reactivity was applied to the synthesis of an unusual dimer linked via the inner carbon atoms of the carbaporphyrinoid rings.[33] However, for most purposes these properties are counterproductive and limit the studies that can be conducted on these systems. With this in mind, the synthesis of carbachlorins and carbaporphyrins with ester groups attached to the carbocyclic rings were targeted for synthesis as it was anticipated that the presence of electron-withdrawing groups would greatly improve the stability of these structures. The synthesis of carbachlorin diester **21** was considered as this could conceivably be derived from cyclopentane dialdehyde **22** (Scheme 2).[34] The required dialdehyde can be prepared from the known Diels-Alder adduct **23** of dimethyl fumarate and cyclopentadiene (Scheme 3). Several different procedures were attempted to prepare norbornene **23**, and superior results were achieved using the method described by Beare *et al.* where freshly cracked cyclopentadiene was gradually added to an aqueous suspension of dimethyl fumarate.[35] Göksu *et al.* had reported that seven bicyclo[2.2.1]heptenes, including **23,** were cleaved to cyclic dialdehydes in good yields by oxidation with $KMnO_4$-$CuSO_4.5H_2O$.[36] However, in our hands all attempts to reproduce this procedure with **23** failed to generate any dialdehyde. Hence, an alternative synthetic method for preparing the required dicarbaldehyde was investigated. The best results were obtained by carrying out a two-step procedure that was adapted from a literature report by Donohoe and coworkers.[37] In this approach, a solution of norbornene **23** in *tert*-butyl alcohol was oxidized with potassium permanganate and sodium hydroxide in *tert*-butyl alcohol and water at 0 ^{o}C to give the *exo*-diol **24** in 73% yield (Scheme 3). Oxidative ring opening of the diol with potassium periodate[30] gave the required dialdehyde **22** in 50% yield. Dialdehyde **22** proved to be very unstable and for this reason was immediately reacted with

tripyrrane dicarboxylic acid **14** in the presence of trifluoroacetic acid (Scheme 4). The solution was neutralized with triethylamine and the solvent removed under reduced pressure. At this stage, a hexahydrocarbaporphyrin intermediate such as **25** may have been generated. The crude product was dissolved in toluene and refluxed with 2-3 equivalents of DDQ in an attempt to form carbachlorin **21**. However, in small scale reactions the only isolatable porphyrinoid product was the related carbaporphyrin **26**. In large scale reactions, carbachlorin **21** could be isolated as a byproduct in up to 10% yield but carbaporphyrin **26** was always observed as the major product in approximately 40% yield. In this respect, the reaction differs from condensations of bicyclic dialdehydes **13** with tripyrrane **14**, as the earlier study only gave carbachlorin products **15** in moderate yields. The presence of a fused five-membered ring in carbachlorins **15** is likely to disfavor oxidation to carbaporphyrin because increased angle strain would result if sp^2 carbons were introduced. Milder conditions for the oxidation were investigated but these experiments either resulted in the formation of little or no isolatable porphyrinoid products, or the predominance of carbaporphyrin **26**. Porphyrinoids **21** and **26** were easily separated by column chromatography on grade 3 alumina. Initially, it had been intended that a related *cis*-carbachlorin isomer would be prepared starting with the Diels-Alder adduct of dimethyl maleate, but as the same carbaporphyrin would be formed and chlorin is only obtained as a minor product, this synthetic variant was not pursued. Although the new methodology does not furnish carbachlorins in acceptable yields, this approach provides a convenient and vastly superior route to a carbaporphyrin that has no ring fused subunits. This has allowed the spectroscopic properties, structural analysis and reactivity of **26** to be explored in detail.

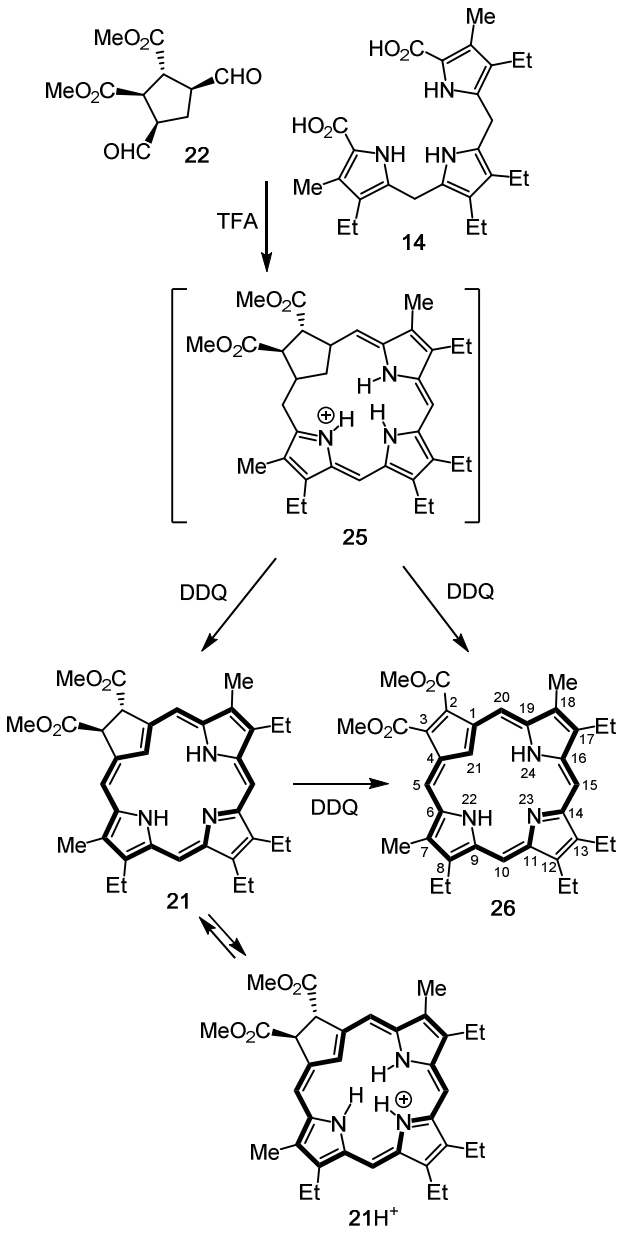

Scheme 4. “3 + 1” synthesis of a carbaporphyrin and a related carbachlorin.

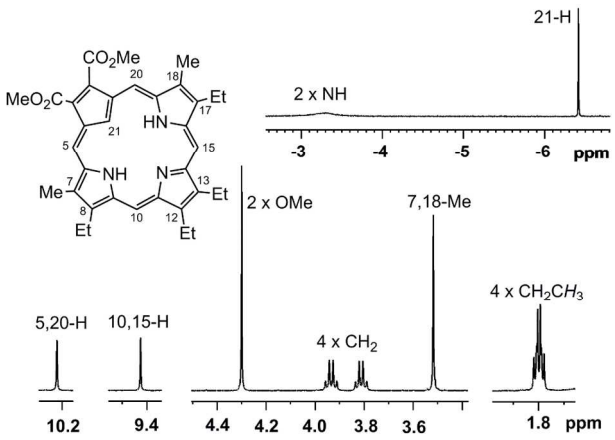

Figure 1. 500 MHz proton NMR spectrum of carbaporphyrin **26** in $CDCl_3$.

As expected, carbaporphyrin **26** proved to be a fully aromatic compound. The proton NMR spectrum in $CDCl_3$ (Figure 1) showed the presence of a strong diatropic ring current, and the internal CH proton was found at -6.27 ppm while the *meso*-protons were shifted downfield to give two 2H singlets at 9.51 and 10.24 ppm. Hence, the difference between the chemical shifts for the internal and external protons ($\Delta\delta$), which is a useful indicator of diatropic character, was just over 16.5 ppm. The 7,18-methyl substituents gave a 6H singlet at 3.51 ppm, showing strong deshielding due to their proximity to the macrocyclic ring current. The carbon-13 NMR spectrum of **26** demonstrated that the macrocycle possesses a plane of symmetry. The *meso*-carbons gave rise to peaks at 94.6 and 107.2 ppm, while the internal carbon afforded a resonance at 100.7 ppm. The UV-Vis spectrum for **26** gave a strong absorption in the Soret region at 436 nm, followed by a series of four weaker Q bands between 520 and 720 nm (Figure 2). These results are typical of aromatic porphyrinoids such as true porphyrins and benzocarbaporphyrins **9a**. High resolution ESI mass spectrometry also supported the identity of **26**. In addition, the structure of carbaporphyrin **26** was confirmed by X-ray crystallography (Figure 3). The molecular structure

shows that the macrocycle is reasonably planar as evidenced by the minimal pyrrole to mean macrocycle plane tilts of 2.24(2)°, 1.13(2)°, and 1.26(2)°. The cyclopentadienyl subunit, however, is significantly tilted 13.63(2)° out of the mean macrocyclic plane. This presumably relieves steric crowding in the central cavity due to the presence of three hydrogen atoms. The three hydrogen atoms, H21, H22 and H24, located in the carbaporphyrin cavity are attached to the parent atoms C(21), and N(22) and N(24), and the pyrrole nitrogen atoms are cis to C(21). Both solution NMR data and solid-state diffraction data are consistent with tautomer **26**, which has two NHs flanking the pyrrolenine nitrogen. With the exception of the unusually short, yet reasonable, C2-C3 bond length, a Mogul geometry check validated all bond distances, angles and torsions to be within typical ranges.[38]

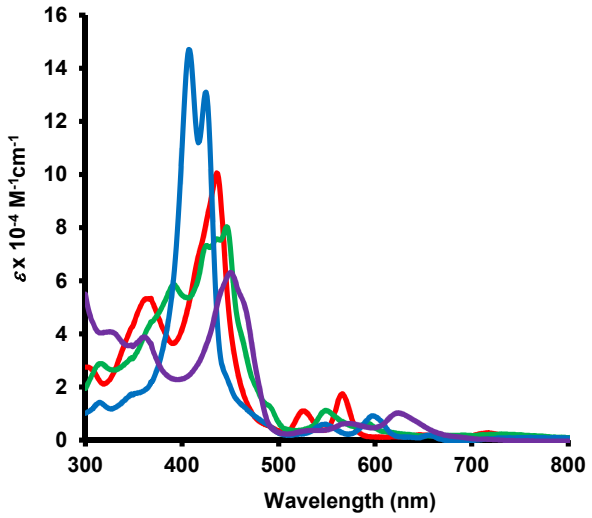

Figure 2. UV-vis spectra of carbaporphyrin **26** in dichloromethane (red line, free base), CH_2Cl_2 with 100 equiv TFA (green line, monocation), 50% TFA-CH_2Cl_2 (blue line, dication) and 5% DBU-CH_2Cl_2 (purple line, monoanion).

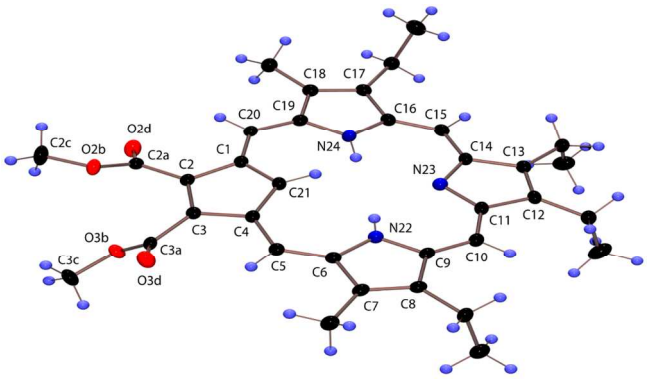

Figure 3 Color POV-Ray rendered ORTEP III drawing (50% probability level, hydrogen atoms rendered arbitrarily small for clarity) of carbaporphyrin **26**.

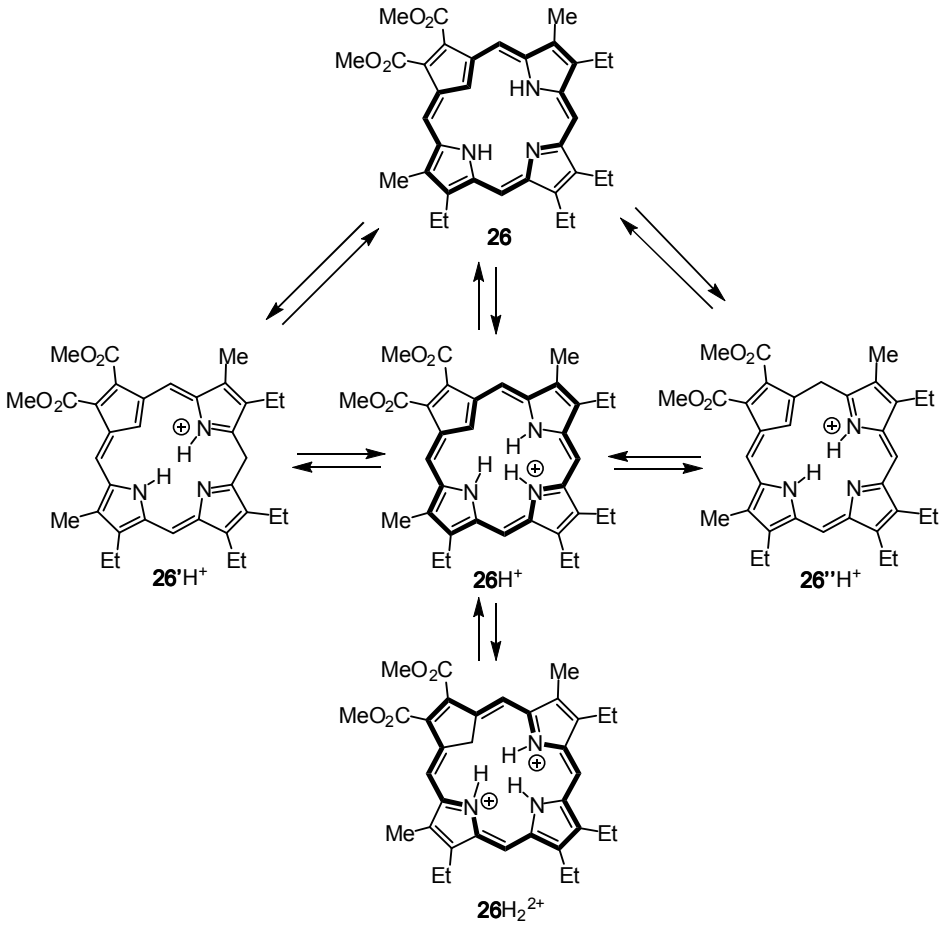

Scheme 5. Protonation and proton exchange for carbaporphyrin **26**.

Upon addition of acid, carbaporphyrin **26** underwent two sequential protonations (Scheme 5). Titration with TFA led to the formation of a new species that was attributed to monocation **26**H^+. Full conversion required the addition of 50 equiv TFA. The UV-Vis spectrum showed multiple weakened Soret bands at 315, 392 and 446 nm and a weaker absorption at 549 nm (Figure 2). In the presence of a large excess of TFA, a *C*-protonated dication **26**H_2^{2+} was generated, and the UV-Vis spectrum for this species in 50% TFA-dichloromethane showed a strong split Soret band at 407 and 425 nm and Q bands at 549, 597 and 656 nm (Figure 2). Addition of one drop of TFA to a NMR tube containing a solution of **26** in $CDCl_3$ resulted in the formation of a mixture of mono- and dicationic species. However, when only 2 μL of TFA was added to the solution, the proton NMR spectrum of the monocation **26**H^+ could be obtained. The *meso*-protons were shifted slightly further downfield to give two 2H singlets at 9.74 and 10.40 ppm. The NH protons gave rise to two broad peaks at -1.97 (2H) and -3.14 (1H) ppm, while the internal CH appeared at -5.95 ppm (Δδ 16.35 ppm). The proton NMR spectrum of the dication in 50% TFA-$CDCl_3$ demonstrated that this species was highly diatropic (Δδ 19.5 ppm) as the internal CH_2 gave an upfield singlet at -7.65 ppm, while the *meso*-protons produced two 2H singlets at 11.10 and 11.86 ppm. The indirect effect of the ring current on the methyl substituents produced 6H singlets for **26**H^+ and **26**H_2^{2+} at 3.44 and 3.79 ppm, respectively, a result that further demonstrates the highly diatropic nature of the dicationic species. Proton and carbon-13 NMR spectra for the mono- and dications confirmed that these structures retain a plane of symmetry.

Addition of d-TFA to an NMR solution of **26** in $CDCl_3$ showed rapid exchange of the 21-H resonance and slow exchange of the *meso*-protons. As the solutions consisted of a mixture of protonated species, it was necessary to extract the sample before NMR analysis could be

conducted. Two drops of d-TFA were added to the NMR tube and after 10 min the solution was neutralized by addition of NaOD in D_2O. The mixture was diluted with water, extracted with dichloromethane and the organic solutions dried over sodium sulfate. Following removal of the solvent, the residue was analyzed by proton NMR spectroscopy. The results showed that the internal CH had undergone exchange but no other resonances were affected. When the solution was exposed to d-TFA for 24 h, and the solution neutralized and extracted as before, significant reductions in the intensities of the *meso*-proton resonances were observed. The peak corresponding to the 5,20-protons was reduced by approximately 15%, while the 10,15-proton resonance was diminished by >40%. The results indicate that *meso*-protonated species such as monocations **26a**H^+ and **26b**H^+ are energetically accessible and in equilibrium with **26**, **26**H^+ and **26**H_2^{2+} (Scheme 5). Similar results have previously been noted for benzocarbaporphyrins.[21b]

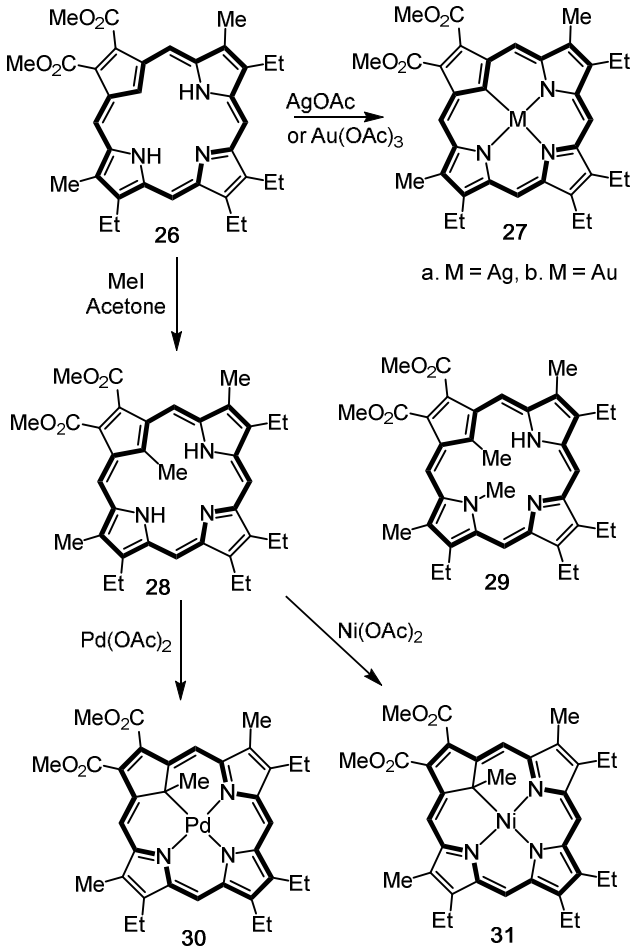

Scheme 6. Alkylation and metalation of carbaporphyrins.

Carbaporphyrinoids, including N-confused porphyrins **5a** and benzocarbaporphyrins **9a**, have previously been shown to form stable silver(III) derivatives.[23,39] Hence, carbaporphyrin diester **26** was treated with silver(I) acetate in methanol-dichloromethane in an attempt to generate the silver(III) complex **27a**. After column chromatography, a red fraction was collected and recrystallized from chloroform-methanol to afford the organometallic complex **27a** as a dark red powder in 60% yield (Scheme 6). Proton NMR spectroscopy demonstrated that silver(III) complex **27a** retained strongly aromatic characteristics as the *meso*-protons showed up as two 2H

singlets at 8.79 and 9.90 ppm. The proton and carbon-13 NMR spectra were also consistent with symmetrical structures. The carbon-13 NMR results showed the *meso*-carbons at 96.1 and 110.1 ppm. The UV-vis spectrum for **27a** produced a Soret-like band at 449 nm together with weaker absorptions at higher and lower wavelength (Figure 4). High resolution ESI MS also confirmed that this species has the molecular formula $C_{35}H_{36}AgN_3O_4$.

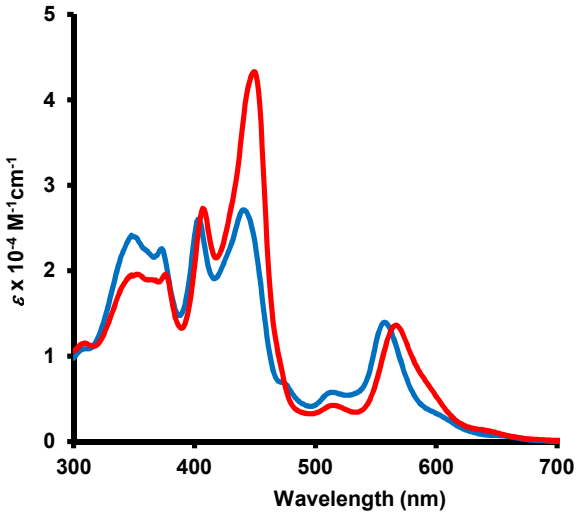

Figure 4. UV-Vis spectra of silver(III) carbaporphyrin **27a** (red line) and gold(III) carbaporphyrin **27b** (blue line) in chloroform.

Gold(III) complexes have previously been prepared by reacting benzocarbaporphyrins such as **9a** with gold(III) acetate, although poor yields were obtained for *meso*-unsubstituted structures.[23b] Attempts to react **26** with gold(III) acetate under the conditions used to prepare the silver(III) complex were unsuccessful and no metalated product could be isolated. However, when **26** was refluxed with gold(III) acetate in pyridine, the solution rapidly changed color from brown to dark red. Following purification by column chromatography and recrystallization from chloroform-methanol, gold(III) complex **27b** was isolated in 44% yield (Scheme 6). Although a

moderate yield was obtained, the electron-withdrawing ester groups do appear to stabilize the carbaporphyrin system to a significant extent and reduce losses due to oxidative decomposition. The gold complex gave a similar UV-vis spectrum (Figure 4) to the silver complex, although the strongest of the Soret bands was significantly reduced in intensity for **27b**. The proton NMR spectrum of **27b** showed significant downfield shifts compared to **27a**. The *meso*-protons appeared 0.09-0.23 ppm further downfield for **27b**, and even the methyl substituents gave a resonance 3.36 ppm for **27b** compared to 3.31 ppm for **27a**.

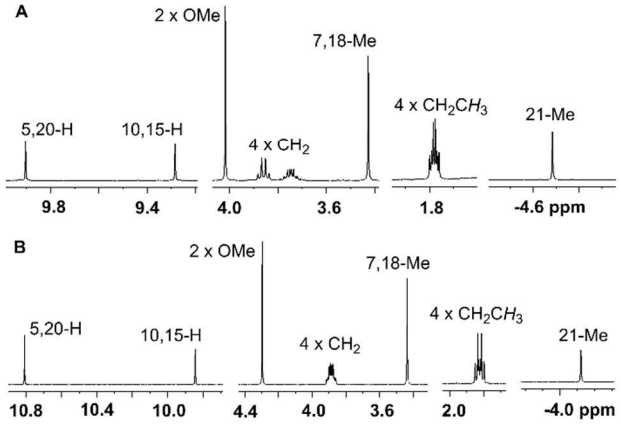

Figure 5. 500 MHz proton NMR spectra of 21-methylcarbaporphyrin **28** (A) and the related palladium(II) complex **30** (B) in $CDCl_3$.

Benzocarbaporphyrin **9a** (R = Et) has previously been shown to react with methyl or ethyl iodide and potassium carbonate in refluxing acetone to afford *N*- and *C*-alkylation products **11a-d**.[25] When carbaporphyrin **26** was reacted with methyl iodide and potassium carbonate in refluxing acetone for 30 min, a single monoalkylation product **28** was obtained in up to 75% yield following purification by column chromatography and recrystallization from chloroform-methanol (Scheme 6). Unexpectedly, the reaction favored substitution at the internal carbon

rather than on the nitrogen atom. Benzocarbaporphyrin **9a** afforded *N*-alkyl derivatives as the major products in these reactions.[25] Although the presence of an internal methyl substituent is likely to reduce the planarity of the macrocycle, the proton NMR spectrum of **28** (Figure 5) showed that the system is highly diatropic and the internal methyl group gave rise to an upfield singlet at -4.68 ppm, while the *meso*-protons were strongly deshielded giving two 2H singlets at 9.28 and 9.90 ppm. Nevertheless, the downfield shifts for the external protons are reduced compared to carbaporphyrin **26** and the methyl resonance shifted upfield by 0.08 ppm The presence of a plane of symmetry was evident from the proton and carbon-13 NMR spectra. In the UV-vis spectrum for the free base, the Soret band was substantially broadened and diminished in intensity giving rise to a peak at 428 nm (Figure 6). A series of Q bands were still present but again these were broadened compared to those observed for **26**. In our studies, UV-vis spectra are commonly run in 1% triethylamine-chloroform, as the additive can scavenge the trace amounts of acid that are commonly associated with chlorinated solvents. However, when **28** was run under these conditions substantial changes in the UV-vis spectrum were observed indicating the formation of a new species that was attributed to monoanion [**28** – H]$^-$ (Scheme 7). It should be noted that the position of the internal NH is not known. In 5% DBU-CH_2Cl_2, full conversion to the monoanion was observed (Figure 6). This spectrum showed three Soret-like bands between 400 and 500 nm and Q bands at 564, 648 and 700 nm. The proton NMR spectrum for **28** in DBU-$CDCl_3$ showed the *meso*-protons downfield at 9.22 and 9.83 ppm, while the internal methyl substituent gave a 3H singlet at -4.78 ppm. Naturally, the aliphatic region was completely obscured by the DBU. The anion is clearly still aromatic and this may be due to the 17-atom 18π electron delocalization pathway shown in structure **A** (Scheme 7). Carbaporphyrin **26** did not

appear to deprotonate with triethylamine but a new species was observed upon addition of DBU (Figure 2).

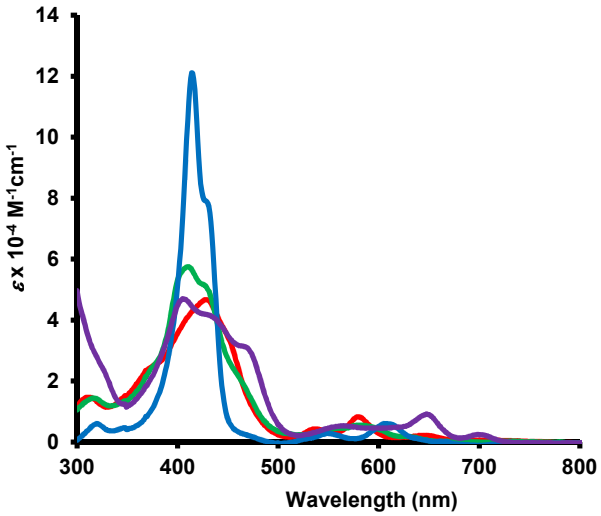

Figure 6. UV-vis spectra of 21-methylcarbaporphyrin **28** in dichloromethane (red line, free base), CH_2Cl_2 with 5 equiv TFA (green line, monocation **28**H^+), 25% TFA-CH_2Cl_2 (blue line, dication **28**H_2^{2+}) and 5% DBU-CH_2Cl_2 (purple line, monoanion).

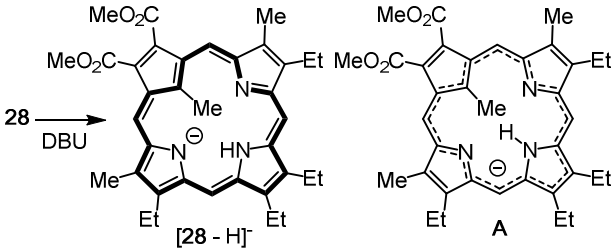

Scheme 7. Deprotonation of carbaporphyrin **28**.

Addition of 5 equiv. of TFA to a solution of *C*-methylcarbaporphyrin **28** led to the formation of monocation **28**H^+(Scheme 8). The UV-Vis spectrum showed a Soret band at 411 nm and broad Q bands between 500 and 650 nm (Figure 6). The proton NMR spectrum for **28**H^+ indicated that this species is slightly more diatropic than the free base form, as the internal

methyl resonance was shifted upfield to -5.41 ppm while the *meso*-protons moved downfield to give two 2H singlets at 9.49 and 10.03 ppm. Further addition of TFA led to the formation of a diprotonated dication **28**H_2^{2+}. In 25% TFA-CH_2Cl_2, the UV-Vis spectrum gave an intense Soret band at 414 nm, with a shoulder at 430 nm, and two broad Q bands at 550 and 606 nm. The proton NMR spectrum for this species in TFA-$CDCl_3$ gave a quartet at -8.67 ppm and a doublet at -6.55 ppm for the 21-H and inner methyl substituent, respectively, while the *meso*-protons showed up at 11.16 and 11.80 ppm. As would be expected, the proton and carbon-13 NMR spectra were both consistent with the mono- and diprotonated structures possessing a plane of symmetry.

When benzocarbaporphyrin **9** was reacted with methyl or ethyl iodide for 16 h, no more than trace amounts of related dialkylation products were observed.[25] However, overnight reactions of **26** with MeI-K_2CO_3 in refluxing acetone afforded a dimethylated derivative **29** as the major product. Following column chromatography and recrystallization from chloroform-methanol, the dialkylated carbaporphyrin **29** was isolated as shiny purple crystals in 69% yield (Scheme 6). The proton NMR spectrum for **29** demonstrated that the methyl groups had been introduced on the inner carbon atom and at an adjacent nitrogen. Crowding due to the presence of two methyl groups within the porphyrinoid core is likely to lead to distortion of the macrocycle but the diamagnetic ring current is only slightly reduced. The internal methyl groups were strongly shifted upfield to give two 3H singlets at -5.27 and -3.91 ppm, while the external *meso*-protons appeared as four 1H singlets at 8.90, 9.05, 9.52 and 9.54 ppm. The external methyl substituents in **29** were not as deshielded as the corresponding resonances for **26** or **28**, and gave rise to two 3H singlets at 2.95 and 3.32 ppm. The duplication of peaks seen in this spectrum demonstrated

that there is no longer a plane of symmetry, and this observation was confirmed by carbon-13 NMR spectroscopy. In addition, as the methyl groups are too large to fit within the cavity, they will both be placed to one side of the structure. It is also likely that the two methyl groups are placed on opposite sides of the macrocycle, and the structure is therefore chiral and exists as a pair of enantiomers. The UV-Vis spectrum for **29** gave broad Soret bands at 376 and 441 nm, two Q bands at 545 and 589 nm, and a broad absorption at 736 nm (Figure 7). The weakened and broadened absorptions again suggest that the system has become somewhat distorted.

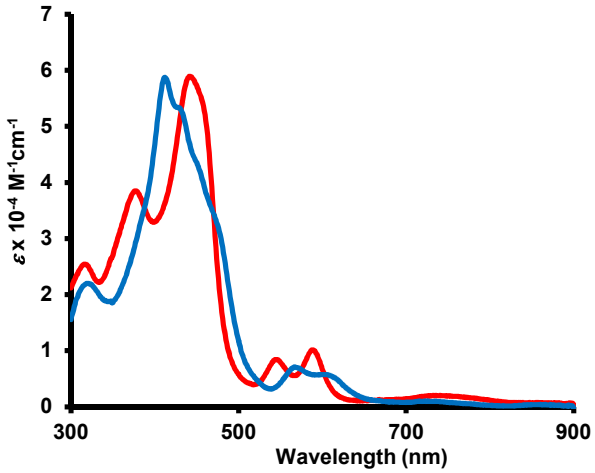

Figure 7. UV-vis spectra of dimethylcarbaporphyrin **29** in 1% Et_3N-CH_2Cl_2 (red line, free base) and in CH_2Cl_2 with 50 equiv. TFA (blue line, monocation **29**H^+).

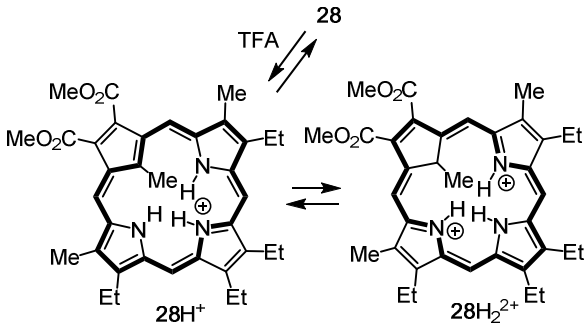

Scheme 8. Protonation of carbaporphyrin **28**.

Addition of trace amounts of TFA led to the formation of monocation **29**H^+, and the UV-Vis spectrum showed a relatively weak Soret band at 412 nm and two broad Q bands at 567 and 607 nm (Figure 7). However, further addition of acid did not generate the related dication and the UV-vis spectrum remained unaltered. Presumably, the steric crowding in the carbaporphyrin cavity inhibits the second protonation. The proton NMR spectrum for monocation **29**H^+ showed the internal methyl resonances at -4.91 and -3.54 ppm, while the *meso*-protons gave four singlets at 9.45, 9.46, 9.86 and 9.92 ppm. The external methyl resonances appeared at 3.03 and 3.37 ppm. The results indicate that the protonated species has a slightly stronger diatropic ring current than the free base form, although the shifts are substantially reduced compared to the original carbaporphyrin **26**.

Metalation of *N*-alkyl benzocarbaporphyrins **9a,c** with palladium(II) acetate in refluxing acetonitrile have previously been shown to give palladium(II) organometallic derivatives **12**.[25] The metalation reaction is associated with an alkyl group migration from the nitrogen to the inner carbon atom. It is noteworthy that the methyl group in **28** is already attached to the internal carbon, and therefore no rearrangement would be necessary to form an analogous palladium complex. In fact, reaction of **28** with palladium(II) acetate in refluxing acetonitrile gave palladium(II) derivative **30** in 63% yield (Scheme 6). Although, the conjugation pathway in the metal complex has been altered, the macrocycle still remains fully aromatic. The proton NMR spectrum of **30** (Figure 5) gave two 2H singlets at 9.85 and 10.81 ppm in the downfield region for the four *meso*-protons, confirming that the complex has a plane of symmetry. Moreover, the presence of a singlet at -4.12 (3H) indicates that the internal methyl group is strongly shielded.

The NMR results show larger upfield and downfield shifts for the palladium complex compared to the free base form of **28** (Figure 5), indicating an enhancement of the diamagnetic ring current. In the carbon-13 NMR spectrum, the internal methyl substituent showed up at 21.8 ppm, while the *meso*-protons gave resonances at 101.7 and 113.0 ppm. The UV-Vis spectrum for **30** gave Soret-like bands at 410 and 460 nm, and a weaker absorption at 602 nm (Figure 8). The structure of palladium complex of carbaporphyrin **30** was also confirmed using X-ray crystallography (Figure 9). The metrics of the framework bond distances are consistent with an overall aromatic carbaporphyrin with an sp^3 hybridized C21. The palladium(II) center resides in a typical square planar coordination environment with 2.054(2) Å Pd-C21, 2.040(2) Å Pd-N22, 2.066(2) Å Pd-N23, and 2.028(1) Å Pd-N24 bond lengths. The framework and metal coordination environment are similar to that of (tetraphenyl-21-formyl-21-carbaporphyrinato)palladium(II)[26] and like this complex, **30** has the palladium(II) ion coordinating η^1 to C21, which being alkylated leads to the distended 1.491(2) Å and 1.495(2) Å $sp^3 \rightarrow sp^2$ C21-C1 and C21-C bond distances. Unlike the relatively short metal to sp^2 formyl carbon atom distance observed in the formyl complex, the sp^3 hybridized C25 methyl group in **30** is not available to interact with the palladium(II) metal center, as illustrated by the over 2.7 Å Pd…C(methyl) separation.

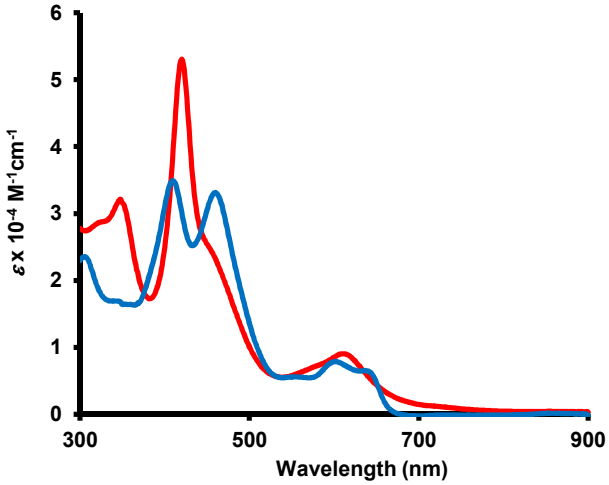

Figure 8. UV-vis spectra of nickel(II) carbaporphyrin **31** (red line) and palladium(II) carbaporphyrin **30** (blue line) in chloroform.

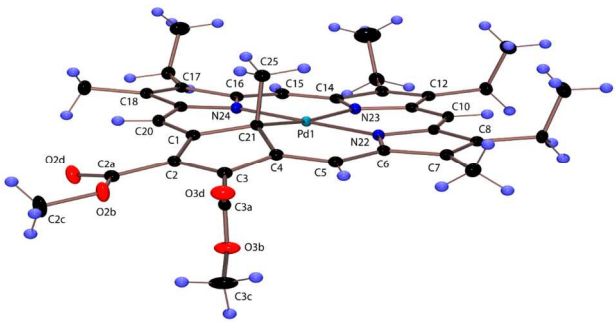

Figure 9. Color POV-Ray rendered ORTEP III drawing (50% probability level, hydrogen atoms rendered arbitrarily small for clarity) of palladium complex **30**

Attempts to react **28** with nickel(II) acetate under the same conditions failed to give the related nickel(II) complex **31** (Scheme 6). However, when the reaction was conducted in refluxing DMF for 30 min, the nickel(II) derivative could be isolated in 70% yield. The proton NMR spectrum of **31** showed two singlets at 9.59 and 10.56 ppm in the downfield region for the four *meso*-protons, and a 3H singlet at -3.89 ppm (3H) for the internal methyl group. Clearly, the macrocycle still retains fully aromatic characteristics and a plane of symmetry. However, the

upfield and downfield shifts for **31** are reduced compared to palladium(II) complex **30**, indicating that **30** can support a slightly larger diamagnetic ring current. The carbon-13 NMR spectrum confirmed the symmetry of this complex and the internal methyl substituent could be identified at 19.8 ppm. The *meso*-carbons gave resonances 2-3 ppm upfield from the values observed for the palladium complex at 99.8 and 111.0 ppm. The identity of the nickel complex, which is the first reported example of a nickel carbaporphyrin, was supported by high resolution ESI MS. The structure was also confirmed by X-ray crystallography (Figure 10). The structure of **31** includes two crystallographically independent residues, the relative bond lengths and angles of which are essentially indistinguishable. The metrics of the framework bond distances are consistent with an overall aromatic carbaporphyrin with an sp^3 hybridized C21. The nickel(II) center resides in a typical square planar coordination environment with 2.02(1) Å Ni-C21, 1.962(2) Å Ni-N22, 1.961(2) Å Ni-N23, and 1.957(2) Å Ni-N24 bond lengths. In fact, the framework and metal coordination environment are very similar to that of (2-aza-tetraphenyl-21-methyl-21-carbaporphyrinato)nickel(II)[40] and (2-aza-tetraphenyl-21-trifluoromethyl-21-carbaporphyrinato)-nickel(II).[41] As is the case for these N-confused porphyrin complexes, **31** has the nickel(II) ion coordinating η^1 to C21, which being methylated leads to the distended 1.48(1) Å $sp^3 \rightarrow sp^2$ C21-C1 and C21-C bond distances.

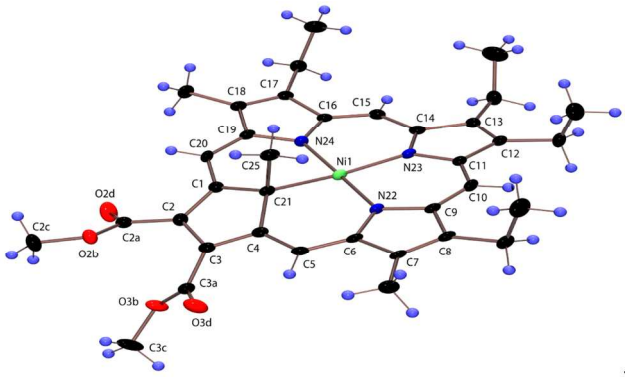

Figure 10. Color POV-Ray rendered ORTEP III drawing (50% probability level, hydrogen atoms rendered arbitrarily small for clarity) of nickel(II) carbaporphyrin **31**.

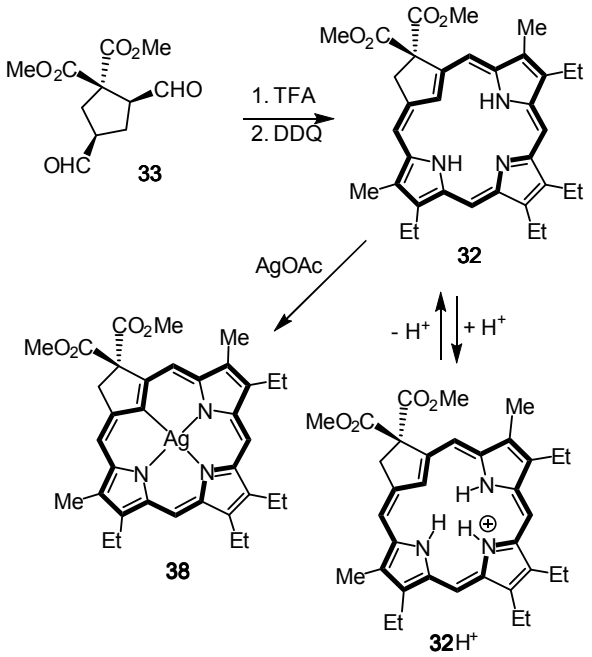

Scheme 9. Synthesis and metalation of carbachlorin **32**.

The reported synthetic strategy provides straightforward access to carbaporphyrins with electron-withdrawing ester groups and has enabled investigations into the spectroscopic properties, protonation, structural characterization and metalation of this important porphyrinoid system. However, the formation of carbachlorin products in respectable yields was thwarted by

the ease with which they were converted to carbaporphyrins. In order to overcome this problem, carbachlorin **32** with geminal diester substituents was targeted for synthesis (Scheme 9). The ester moieties are placed in a fashion that would block further oxidation to carbaporphyrin and thereby open up carbachlorins for more detailed studies. The plan necessitated access to cyclopentane dialdehyde **33**, and this intermediate was obtained from norbornene **34** using a similar strategy to the one used to prepare dialdehyde **22**. The required norbornene diester **34** could be generated by a Diels-Alder cycloaddition reaction using dienophile **35** (Scheme 10). Dimethyl 1,1-ethylenedicarboxylate (**35**) was prepared by a literature procedure reported by Takayama and coworkers[42] by reacting copper(II) acetate in glacial acetic acid with paraformaldehyde and dimethyl malonate. Due to the high reactivity of **35**, it was immediately diluted with dichloromethane and reacted with cyclopentadiene to give the bicyclic adduct **34**. Following purification by column chromatography on silica gel, norbornene **34** was isolated as a colorless oil in 80% yield (Scheme 10). Oxidation with potassium permanganate and sodium hydroxide in water and *tert*-butyl alcohol afforded the required *exo*-dialcohol **36** as a white crystalline solid in 61% yield. Oxidative ring-opening with potassium periodate gave the unstable dialdehyde **33** in 60% yield (Scheme 10). Due to its instability, **33** was immediately condensed with tripyrrane dicarboxylic acid **14** in the presence of TFA in dichloromethane. Subsequent oxidation with DDQ in refluxing toluene afforded carbachlorin **32** in 30% yield (Scheme 9).

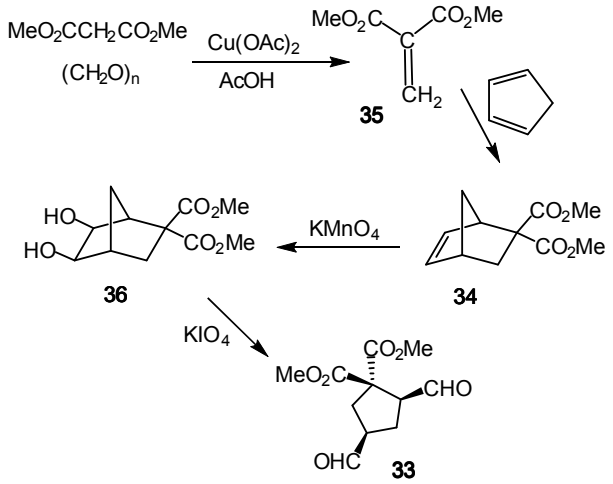

Scheme 10. Synthesis of a cyclopentane dialdehyde with two geminal ester substituents.

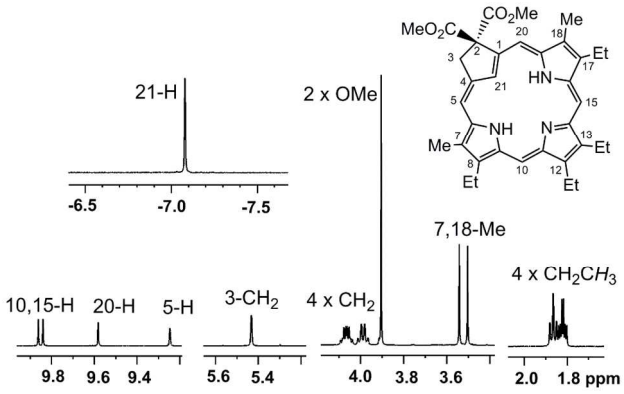

Figure 11. 500 MHz proton NMR spectrum of carbachlorin **32** in $CDCl_3$.

Carbachlorin **32**, like other chlorin analogues, proved to be a fully aromatic system. The proton NMR spectrum for **32** in $CDCl_3$ (Figure 11) showed the presence of a strong diamagnetic ring current and the internal CH proton was found at -7.08 ppm, while the *meso*-protons shifted downfield to give four 1H singlets at 9.25, 9.58, 9.84 and 9.86 ppm ($\Delta\delta$ 16.94 ppm). The methyl substituents were also significantly deshielded by the ring current effect, giving rise to two 3H

singlets at 3.50 and 3.54 ppm. Due to the placement of the ester moieties, the macrocycle is no longer symmetrical. In the carbon-13 NMR spectrum, the *meso*-carbons appeared at 96.2, 96.5, 97.7 and 99.3 ppm, and the internal carbon was identified at 120.7 ppm. The UV-Vis spectrum of carbachlorin **32** gave a strong Soret band at 398 nm, along with smaller Q bands at 491, 588 and 646 nm (Figure 12). It is noteworthy that the long wavelength absorption band at 646 nm, which is a characteristic feature of chlorin-type structures, has undergone a small hypsochromic shift due to the presence of the electron-withdrawing ester substituents. The structure of **32** was further confirmed by X-ray crystallography (Figure 13). While substantial disorder of the main residue precluded a detailed metric analysis, the presence of a geminal diester on C2 is evident.

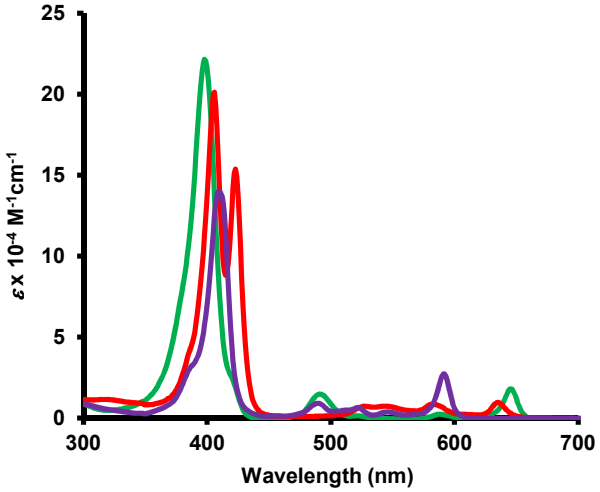

Figure 12. UV-vis spectra of carbachlorin **32** in dichloromethane (green line), carbachlorin monocation **32**H^+ in 5% TFA-dichloromethane (red line) and silver(III) carbachlorin **38** in dichloromethane (purple line).

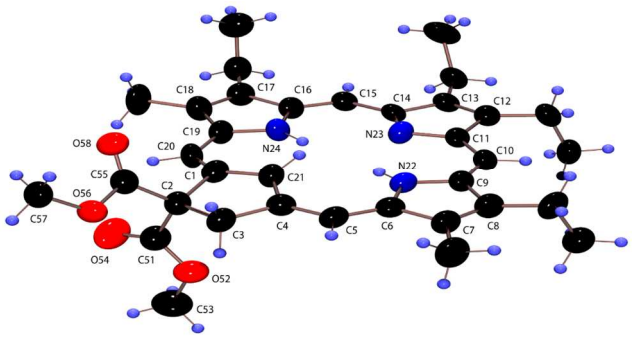

Figure 13 Color POV-Ray rendered ORTEP III drawing (50% probability level, hydrogen atoms rendered arbitrarily small for clarity; disorder suppressed) of carbachlorin **32**.

When carbachlorin **32** was exposed to a trace amount of TFA, a deep purple solution corresponding to monocation **32**H$^+$ (Scheme 9) was generated. The UV-Vis spectrum for **32**H$^+$ gave an intense split Soret band at 406 and 423 nm and Q bands at 527, 543, 583 and 635 nm (Figure 12). The proton NMR spectrum for **32**H$^+$ indicated a slight enhancement of the aromatic character, as the internal CH moved upfield to -7.10 ppm while the *meso*-protons were shifted further downfield to give four singlets at 9.71, 9.96, 10.226 and 10.231 ppm ($\Delta\delta$ 17.33 ppm). The appearance of broad singlets at -4.95 ppm (2H) and -5.96 ppm (1H) confirmed the presence of an additional NH due to protonation. The carbon-13 NMR spectrum showed the *meso*-carbons at 94.6, 94.7, 103.7 and 103.9 ppm, while the internal carbon was observed at 128.6 ppm. Unlike the related carbaporphyrins, further addition of TFA to **32**H$^+$ did not give a diprotonated species, as the aromatic character would be disrupted if protonation occurred at the inner carbon atom.

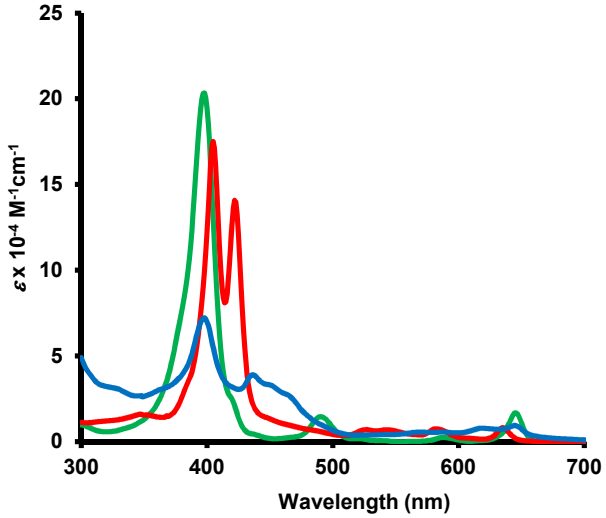

Figure 14. UV-vis spectra of carbachlorin by-product **21** in dichloromethane (green line, free base), 5% TFA-dichloromethane (red line, monocation **21**H^+) and 5% DBU-dichloromethane (blue line).

Carbachlorin by-product **21** was also fully characterized. The proton NMR spectrum for **21** in $CDCl_3$ again showed the presence of a strong diamagnetic ring current, and the internal CH proton was located upfield at -7.14 ppm, while the *meso*-protons were strongly deshielded giving two 2H singlets at 9.48 and 9.85 ppm (Δδ 17.0 ppm). The rotational symmetry anticipated for this structure reduced the number of peaks observed in the proton and carbon-13 NMR spectra. The UV-Vis spectrum gave a Soret band at 405 nm and Q bands at 490, 588 and 645 nm (Figure 14). Addition of TFA to solutions of **21** gave rise to deep purple solutions of the corresponding monocation **21**H^+ (Scheme 4). The UV-Vis spectrum in 5% TFA-CH_2Cl_2 gave a split Soret band at 405 and 422 nm and Q bands at 527, 582 and 635 nm (Figure 14). The proton NMR spectrum for **21**H^+ in TFA-$CDCl_3$ again showed the internal CH near -7 ppm, while the *meso*-protons were shifted downfield to give two 2H singlets at 9.84 and 10.30 ppm (Δδ 17.26 ppm). Addition of DBU to solution of carbachlorin **32** did not result in the formation of a new anionic species.

However, in 5% DBU-CH_2Cl_2, the UV-vis spectrum of **21** was highly modified showing a Soret-like band at 398 nm and broad absorptions between 450 and 700 nm (Figure 14). It is speculated that this new species may has arisen from deprotonation of the carbocyclic ring to form an enolate ion **37** (Scheme 11). This transformation is not possible for carbachlorin **32**.

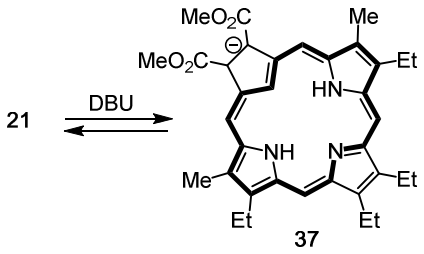

Scheme 11. Deprotonation of carbachlorin **21**.

When d-TFA was added to a solution of **32** in $CDCl_3$ the resulting monocation did not show any exchange of the inner CH proton, in contrast to carbaporphyrins which exhibit rapid deuterium exchange. However, exchange of the *meso*-protons was evident. After 20 min, the intensities for two of the *meso*-resonances were reduced by 15%, while the remaining two peaks were reduced by more than 50%. After several hours, proton-deuterium exchange was virtually 100% for all four *meso*-positions. The results imply that *meso*-substituted monocations such as **32a-d**H^+ are in equilibria with **32** and **32**H^+ (Scheme 12). It is possible that related dications could also be involved. It is noteworthy that the exchange rate for the *meso*-protons in chlorin **32** is far greater than the exchange rates noted for carbaporphyrins such as **26**. The results also show that the 5,20-protons exchange more rapidly than the 10,15-protons. Addition of d-TFA to a solution of carbachlorin **21** similarly showed exchange at the *meso*-positions, albeit at a slightly

slower rate. Again, exchange of the 5,20-protons occurred more rapidly than for the 10,15-protons.

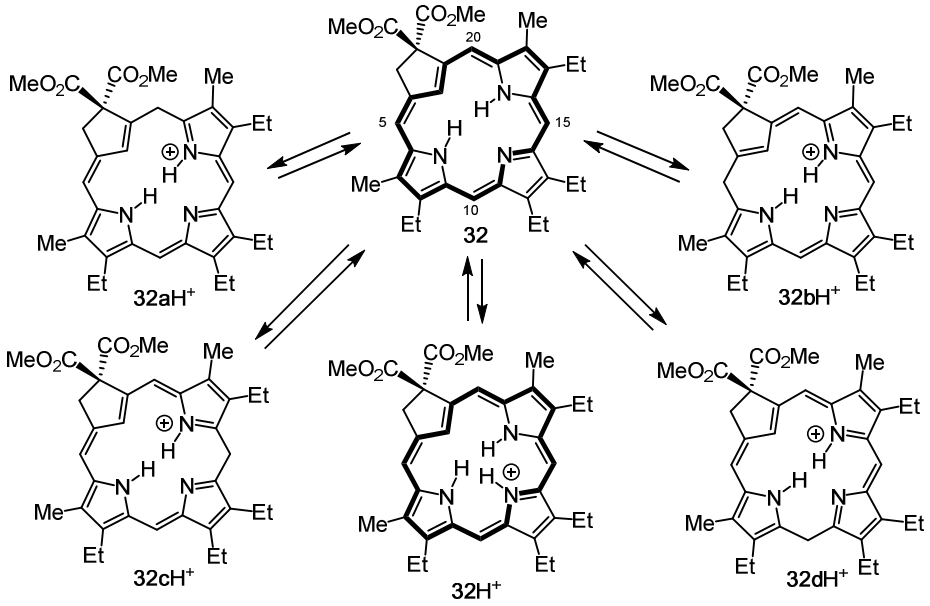

Scheme 12. Proton exchange for carbachlorin monocations.

Metalation of carbachlorin **32** with silver(I) acetate was also investigated. A solution of carbachlorin **32** in dichloromethane was added to a suspension of silver(I) acetate in methanol, and the resulting mixture was stirred overnight at room temperature. Purification by column chromatography gave a red fraction that was recrystallized from chloroform-methanol to yield the organometallic complex **38** as a dark red powder in 82% yield (Scheme 9). The UV-Vis spectrum of **38** (Figure 12) gave a strong Soret band at 410 nm, along with four smaller absorptions at 490, 522, 546 nm and 592 nm. The longest wavelength band is relatively strong, as would be expected for a metallochlorin analogue. The proton NMR spectrum for silver(III) complex **38** showed that the macrocycle remained highly diatropic and the *meso*-protons were shifted downfield to give four 1H singlets at 9.36, 9.70, 9.93 and 9.98 ppm. The carbon-13 NMR

spectrum showed the *meso*-carbons at 98.2, 98.5, 101.3 and 103.0 ppm. The identity of **38** was further confirmed by high resolution ESI MS.

Conclusions

Carbachlorins and carbaporphyrins with electron-withdrawing ester functionalities have been prepared in superior yields using MacDonald-type "3 + 1" syntheses. The required dialdehyde intermediates were conveniently obtainable from the Diels-Alder adducts of dimethyl fumarate or dimethyl 1,1-ethylenedicarboxylate with cyclopentadiene. The presence of electron-withdrawing substituents further stabilized these structures and enabled the reactivity of these systems to be investigated. The carbaporphyrin readily formed a silver(III) complex and gave moderate yields of a related gold(III) derivative. Alkylation with methyl iodide was favored at the internal carbon, but prolonged reaction times led to the formation of a 21,22-dimethylcarbaporphyrin. The 21-methylcarbaporphyrin reacted with palladium(II) and nickel(II) acetate to afford organometallic derivatives where the metal cations were covalently bound to an sp^3 hybridized carbon atom and the internal methyl groups were pivoted at virtually right angles relative to the macrocyclic plane. By using a cyclopentane dialdehyde with geminal diester units, the "3 + 1" strategy gave a novel carbachlorin. This porphyrinoid had highly diatropic characteristics and reacted with silver(I) acetate to give a silver(III) carbachlorin. Carbachlorins have moderately strong absorptions between 645 and 650 nm and this property may be benefical in the development of new photosensitizers for PDT applications.

EXPERIMENTAL SECTION

Melting points are uncorrected. NMR spectra were recorded using a 400 or 500 MHz NMR spectrometer and were run at 300 K unless otherwise indicated. ^{1}H NMR values are reported as chemical shifts δ, relative integral, multiplicity (s, singlet; d, doublet; t, triplet; q, quartet; p, pentet; m, multiplet; br, broad peak) and coupling constant (*J*). Chemical shifts are reported in parts per million (ppm) relative to $CDCl_3$ (^{1}H residual $CHCl_3$ δ 7.26, ^{13}C $CDCl_3$ triplet δ 77.23) and coupling constants were taken directly from the spectra. NMR assignments were made with the aid of ^{1}H-^{1}H COSY, HSQC, DEPT-135 and nOe difference proton NMR spectroscopy. 2D experiments were performed by using standard software. High-resolution mass spectra (HRMS) were carried out by using a double focusing magnetic sector instrument. ^{1}H and ^{13}C NMR spectra for all new compounds are reported in Supporting Information.

Dimethyl bicyclo[2.2.1]hept-5-ene-2-*endo*-3-*exo*-dicarboxylate (**23**).[43] Freshly cracked cyclopentadiene (6.6 mL, 78 mmol) was added to a suspension of dimethyl fumarate (10.0 g, 69.3 mmol) in water (400 mL) and the suspension was stirred vigorously for 120 min. Ethyl acetate (150 mL) was added, and the phases were separated, the organic layer dried over sodium sulfate and the solvent evaporated under reduced pressure to give the title compound (10.7 g, 50.9 mmol, 73%) as a colorless oil. ^{1}H NMR (500 MHz, $CDCl_3$): δ 1.46 (1H, dq, *J* = 8.8, 1.7 Hz), 1.62 (1H, br t, *J* = 8.8 Hz), 2.69 (1H, dd, *J* = 4.5, 1.7 Hz), 3.11-3.14 (1H, m), 3.25-3.28 (1H, m), 3.38 (1H, t, *J* = 4.1 Hz), 3.65 (3H, s), 3.72 (3H, s), 6.07 (1H, dd, *J* = 5.6, 2.8 Hz), 6.28 (1H, dd, *J* = 5.6, 3.1 Hz). ^{13}C NMR (125 MHz, $CDCl_3$): δ 45.9, 47.3, 47.5, 47.8, 48.1, 52.0, 52.3, 135.4, 137.8, 173.9, 175.1.

Dimethyl bicyclo[2.2.1]hept-5-en-2,2-dicarboxylate (**34**).[44] Dimethyl 1,1-ethylenedicarboxylate[42] (1.37 g, 0.021 mol) was added slowly to freshly cracked 1,3-

cyclopentadiene (3.00 g, 0.021 mol) whilst stirring and maintaining the temperature at 25 °C with the aid of a water bath. The reaction mixture was stirred at room temperature for 60 min and purified by column chromatography on silica gel eluting with ethyl acetate-hexane (1:19) to give the diester (2.97 g, 0.0141 mmol, 80%) as a colorless oil. ^{1}H NMR (500 MHz, $CDCl_3$): δ 1.48-1.52 (1H, m), 1.65 (1H, br d, *J* = 8.9 Hz), 1.99 (1H, dd, *J* = 12.4, 2.9 Hz), 2.10 (1H, dd, *J* = 12.4, 3.6 Hz), 2.90 (1H, br), 3.37-3.39 (1H, br m), 3.65 (3H, s), 3.72 (3H, s), 5.97 (1H, dd, *J* = 5.6, 2.9 Hz), 6.24 (1H, dd, *J* = 5.6, 3.1 Hz). ^{13}C NMR (125 MHz, $CDCl_3$): δ 36.1, 42.2, 48.9, 50.0, 52.5, 52.9, 60.4, 133.7, 140.0, 171.6, 173.2. HRMS (EI): calcd for $C_{11}H_{14}O_4$ 210.0892, found 210.0896.

Dimethyl 5,6-dihydroxybicyclo[2.2.1]heptane-2,3-dicarboxylate (**24**). A solution of potassium permanganate (12.0 g, 76.0 mmol) and sodium hydroxide (2.61 g, 65.3 mmol) in water (250 mL) was added to a solution of norbornene **23** (10.83 g, 51.5 mmol) in *tert*-butyl alcohol (200 mL) and water (50 mL) at 0 °C. After the addition was complete, the mixture was stirred for 20 min and then quenched with a saturated aqueous solution of sodium metabisulfite until the solution turned colorless. The mixture was filtered and the *tert*-butyl alcohol was removed from the filtrate *in vacuo*. The solution was extracted with ethyl acetate (4 x 100 mL) and the combined organic layers dried over magnesium sulfate, filtered and concentrated *in vacuo* to furnish the diol (6.85 g, 28.0 mmol, 55%) as a white crystalline solid, mp 84-86 °C (lit. mp[45] 81-84 °C; 89.9-92.3 °C[46]). ^{1}H NMR (500 MHz, $CDCl_3$): δ 1.44 (1H, dp, *J* = 11.0, 1.5 Hz), 1.89 (1H, dq, *J* = 11.0, 1.5 Hz), 2.50 (1H, br s), 2.55-2.57 (1H, m), 2.62 (1H, br), 2.73 (1H, br s overlapping with dd, *J* = 5.7, 1.3 Hz), 3.20 (1H, t, *J* = 5.1 Hz), 3.70 (3H, s), 3.71 (3H, s), 3.76-3.79 (1H, br m), 3.86-3.89 (br m). ^{13}C NMR (125 MHz, $CDCl_3$): δ 31.9, 45.0, 46.4, 46.7, 48.5,

52.4, 52.5, 70.6, 73.7, 173.1, 174.2. HRMS (EI): calcd for $C_{11}H_{16}O_6$ + H 245.1025, found 245.1027.

Dimethyl *exo*-5,6-dihydroxybicyclo[2.2.1]heptane-2,2-dicarboxylate (**36**). Using the previous procedure, norbornene **34** (10.80 g, 53.1 mol) in *tert*-butyl alcohol (200 mL) and water (50 mL) was reacted with potassium permanganate (12.0 g, 76.0 mol) and sodium hydroxide (2.61 g, 65.3 mmol) in water (250 mL) to furnish diol **36** (6.23 g, 0.025 mmol, 61%) as a white crystalline solid, mp 82-84 ^{o}C. ^{1}H NMR (500 MHz, $CDCl_3$): δ 1.43 (1H, dp, *J* = 11.0, 1.6 Hz), 1.88 (1H, dq, *J* = 11.0, 1.6 Hz), 2.49-2.50 (1H, m), 2.54-2.56 (1H, m), 2.72 (1H, dd, *J* = 5.6, 1.5 Hz), 2.86 (1H, br), 2.96 (1H, br), 3.20 (1H, dd, *J* = 5.6, 4.7 Hz), 3.69 (3H, s), 3.71 (3H, s), 3.75-3.77 (1H, m), 3.85-3.87 (1H, m). ^{13}C NMR (125 MHz, $CDCl_3$): δ 31.9, 45.0, 46.4, 46.7, 48.5, 52.4, 52.5, 70.5, 73.6, 173.2, 174.3. HRMS (EI): calcd for $C_{11}H_{16}O_6$ + H 245.1025, found 245.1017.

8,12,13,17-Tetraethyl-2,3-dimethoxycarbonyl-7,18-dimethyl-21-carbaporphyrin (**26**). Diol **24** (4.15 g, 16.9 mmol) was mixed with water (5.0 mL), diethyl ether (10 mL) and potassium periodate (4.66 g, 20.3 mmol) and the mixture stirred at room temperature for 1 h. The remaining solid was filtered off and the two phases were separated. The water layer was extracted twice with ether, and the combined organic layers were dried over sodium sulfate and the solvent removed under reduced pressure to give dialdehyde **22** (2.08 g, 8.59 mmol, 50%) as a clear oil. The unstable dialdehyde was not further purified but used immediately to prepare carbaporphyrin. ^{1}H NMR (400 MHz, $CDCl_3$): 2.17-2.26 (1H, m), 2.46 (1H, dt, *J* = 13.8, 5.9 Hz), 3.05-3.10 (1H, m), 3.26-3.32 (1H, m), 3.56-3.65 (2H, m), 3.70 (3H, s), 3.76 (3H, s), 9.65 (1H, d, *J* = 0.8 Hz), 9.68 (1H, d, *J* = 0.9 Hz). HRMS (EI): calcd for $C_{11}H_{14}O_6$ + H 243.0869, found 243.0871.

Tripyrrane dicarboxylic acid **14** (100 mg, 0.22 mmol) was stirred with TFA (1 mL) under an atmosphere of nitrogen for 2 min in a 250 mL round bottom flask. Dichloromethane (99 mL) was added, followed immediately by dialdehyde **22** (56 mg, 0.23 mmol), and the mixture was stirred under nitrogen overnight. The mixture was neutralized by the addition of triethylamine and the solvent removed under reduced pressure, then the residue was taken up in toluene (50 mL), DDQ (150 mg, 0.66 mmol) was added and the resulting mixture stirred under reflux for 1 h. The solvent was removed under reduced pressure, and the residue dissolved in dichloromethane and washed with water. The solvent was evaporated under reduced pressure and the residue chromatographed on grade 3 neutral alumina eluting with 60:40 dichloromethane-hexanes. Following an initial red fraction, a major dark brown fraction corresponding to the carbaporphyrin was collected. Recrystallization from chloroform-methanol gave carbaporphyrin **26** (52 mg, 0.092 mmol, 42%) as purple crystals, mp 234-236 ^{o}C. UV-Vis (1% Et_3N-CH_2Cl_2): λ_{max} (log ε) 368 (4.73), 436 (5.00), 526 (4.04), 566 (4.24), 648 (3.31), 717 nm (3.43). UV-Vis (5% DBU-CH_2Cl_2): λ_{max} (log ε) 361 (4.59), 450 (4.80), 530 (sh, 3.55), 572 (sh, 3.80), 625 nm (4.01). UV-Vis (100 eq TFA-CH_2Cl_2): λ_{max} (log ε) 315 (4.46), 392 (4.77), 446 (4.91), 549 nm (4.05). UV-Vis (50% TFA-CH_2Cl_2): λ_{max} (log ε) 315 (4.15), 407 (5.17), 425 (5.12), 549 (3.79), 597 (3.96), 656 nm (3.27). ^{1}H NMR (500 MHz, $CDCl_3$): δ -6.27 (1H, s, 21-H), -3.12 (2H, br, 2 x NH), 1.77-1.83 (12H, 2 overlapping triplets, 4 x CH_2CH_3), 3.51 (6H, s, 7,18-Me), 3.84 (4H, q, J = 7.6 Hz, 12,13-CH_2), 3.95 (4H, q, J = 7.6 Hz, 7,18-CH_2), 4.27 (6H, s, 2 x OMe), 9.51 (2H, s, 10,15-H), 10.24 (2H, s, 5,20-H). ^{13}C NMR (125 MHz, $CDCl_3$): δ 11.5 (7,18-Me), 17.3 (8,17-CH_2CH_3), 18.4 (12,13-CH_2CH_3), 19.5 (8,17-CH_2), 19.9 (12,13-CH_2), 52.6 (2 x OMe), 94.6 (10,15-CH), 100.7 (21-CH), 107.2 (5,20-CH), 130.5, 131.6, 135.5, 136.0, 137.7,

139.4, 145.4, 156.1, 167.6 (2 x C=O). ^{1}H NMR (500 MHz, 2 µl TFA-$CDCl_3$): δ -5.95 (1H, s), -3.14 (1H, v br, 23-NH), -1.97 (2H, s, 22,24-NH), 1.65 (6H, t, *J* = 7.6 Hz, 8,17-$CH_2C\mathit{H}_3$), 1.80 (6H, t, *J* = 7.6 Hz, 12,13-$CH_2C\mathit{H}_3$), 3.44 (6H, s, 7,18-Me), 3.90-4.00 (8H, 2 overlapping quartets, 4 x $C\mathit{H}_2CH_3$), 4.26 (6H, s, 2 x OMe), 9.74 (2H, s, 10,15-CH), 10.40 (2H, s, 5,20-CH). ^{13}C NMR (125 MHz, 2 µl TFA-$CDCl_3$): δ 11.7 (7,18-Me), 16.6 (8,17-$CH_2\mathit{C}H_3$), 17.4 (12,13 $CH_2\mathit{C}H_3$), 19.78, 19.81 (4 x CH_2), 53.2 (2 x OMe), 94.2 (10,15-CH), 111.8, 113.8 (5,20-CH), 132.7, 134.1, 138.5, 140.2, 140.4, 140.5, 141.5, 142.9, 167.3 (2 x C=O). ^{1}H NMR (500 MHz, 50% TFA-$CDCl_3$): δ -7.65 (1H, s), 1.82 (12H, t, *J* = 7.6 Hz, 4 x $CH_2C\mathit{H}_3$), 3.79 (6H, s, 7,18-Me), 4.22-4.32 (8H, m, 4 x $C\mathit{H}_2CH_3$), 4.69 (6H, s, 2 x OMe), 11.10 (2H, s, 10,15-CH), 11.86 (2H, s, 5,20-H). ^{13}C NMR (125 MHz, 50% TFA-$CDCl_3$): δ 11.7 (7,18-Me), 16.3 (2 x $CH_2\mathit{C}H_3$), 17.4 (2 x $CH_2\mathit{C}H_3$), 20.6 (4 x $\mathit{C}H_2CH_3$), 29.2 (21-CH), 55.5 (2 x OMe), 105.1 (10,15-CH), 115.0 (5,20-CH), 142.7, 144.1, 144.8, 146.1, 147.1, 148.2, 148.2, 148.3, 149.0, 149.3, 167.3 (2 x C=O). HRMS (ESI): calcd for $C_{35}H_{39}N_3O_4$ + H 566.3019, found 566.3047.

***trans*-8,12,13,17-Tetraethyl-2,3-dimethoxycarbonyl-7,18-dimethyl-2,3-dihydro-21-carbaporphyrin** (**21**). A third dark green fraction was also collected from the previous reaction and subsequent recrystallization from chloroform-methanol gave a carbachlorin by-product (12 mg, 0.021 mmol, 9.6%) as a green powder, mp 232-234 °C; UV-Vis (CH_2Cl_2): λ_{max} (log ε) 398 (5.31), 490 (4.17), 588 (3.41), 645 nm (4.23). UV-Vis (5% TFA-CH_2Cl_2): λ_{max} (log ε) 348 (4.21), 405 (5.24), 422 (5.15), 527 (3.84), 544 (sh, 3.84), 582 (3.88), 635 nm (3.91). UV-Vis (5% DBU-CH_2Cl_2): λ_{max} (log ε) 398 (4.86), 437 (4.59), 450 (sh, 4.52), 464 (sh, 4.44), 569 (sh, 3.74), 587 (sh, 3.75), 619 (sh, 3.90), 645 nm (sh, 3.98). ^{1}H NMR (500 MHz, $CDCl_3$): δ -7.14 (1H, s, 21-H), 1.82 (6H, t, *J* = 7.7 Hz, 8,17-$CH_2C\mathit{H}_3$), 1.86 (6H, t, *J* = 7.7 Hz, 12,13-$CH_2C\mathit{H}_3$), 3.53 (6H, s,

7,18-Me), 3.92 (6H, s, 2 x OMe), 3.98 (4H, q, J = 7.7 Hz, 12,13-CH_2), 4.06 (4H, q, J = 7.7 Hz, 8,17-CH_2), 6.34 (2H, s, 2,3-H), 9.48 (2H, s, 5,20-H), 9.85 (2H, s, 10,15-H). ^{13}C NMR (125 MHz, $CDCl_3$): δ 11.5 (7,18-Me), 17.6 (8,17-CH_2CH_3), 18.8 (12,13-CH_2CH_3), 19.8 (8,17-CH_2), 20.1 (12,13-CH_2), 53.0 (2 x OMe), 56.0 (2,3-CH), 96.6 (10,15-CH), 97.9 (5,20-CH), 119.7 (21-CH), 130.0, 133.0, 135.7, 138.0, 139.6, 143.4, 150.5, 173.7. ^{1}H NMR (500 MHz, TFA-$CDCl_3$): δ -6.96 (1H, s, 21-H), -6.00 (1H, br s, 23-NH), -5.56 (2H, br s, 22,24-NH), 1.72 (6H, t, J = 7.7 Hz, 8,17-CH_2CH_3), 1.82 (6H, t, J = 7.7 Hz, 12,13-CH_2CH_3), 3.53 (6H, s, 7,18-Me), 4.01 (6H, s, 2 x OMe), 4.12 (4H, q, J = 7.7 Hz, 8,17-CH_2), 4.19 (4H, q, J = 7.7 Hz, 12,13-CH_2), 6.34 (2H, s, 2,3-H), 9.84 (2H, s, 5,20-H), 10.30 (2H, s, 10,15-H). ^{13}C NMR (125 MHz, TFA-$CDCl_3$): δ 11.4 (7,18-Me), 16.6 (8,17-CH_2CH_3), 17.5 (12,13-CH_2CH_3), 20.2 (2 x CH_2CH_3), 20.3 (2 x CH_2CH_3), 54.8 (2 x OMe), 56.9 (2,3-CH), 94.9 (10,15-CH), 103.3 (5,20-CH), 128.4 (21-CH), 134.8, 135.2, 136.2, 141.7, 142.3, 142.8, 143.3, 176.1 (2 x C=O). HRMS (ESI): calcd for $C_{35}H_{41}N_3O_4$ + H 568.3175, found 568.3181.

8,12,13,17-Tetraethyl-2,2-dimethoxycarbonyl-7,18-dimethyl-2,3-dihydro-21-carbaporphyrin (**32**). Using the foregoing conditions, diol **36** (3.05 g, 0.021 mol) was reacted with potassium periodate (4.16 g, 0.018 mol) in water (5 mL) and ether (10 mL) to afford dialdehyde **33** (1.67 g, 0.021 mmol, 60%) as a clear oil. The unstable dialdehyde was not further purified but used immediately to prepare carbachlorin. ^{1}H NMR (400 MHz, $CDCl_3$): 2.17-2.25 (1H, m), 2.47 (1H, dt, J = 13.8, 5.9 Hz), 3.05-3.11 (1H, m), 3.27-3.32 (1H, m), 3.57-3.66 (2H, m), 3.70 (3H, s), 3.76 (3H, s), 9.65 (1H, d, J = 0.8 Hz), 9.68 (1H, d, J = 0.9 Hz). HRMS (EI): calcd for $C_{11}H_{14}O_6$ + H 243.0869, found 243.0870.

Tripyrrane dicarboxylic acid **14** (100 mg, 0.22 mmol) was reacted with dialdehyde **33** (55 mg, 0.23 mmol) and oxidized with DDQ (100 mg, 0.44 mmol) as described above. The crude product was purified by column chromatography on neutral grade 3 alumina eluting 60:40 dichloromethane-hexanes and the carbachlorin was collected as a dark green fraction. Recrystallization from chloroform-methanol gave **32** (37 mg, 0.065 mmol, 30%) as purple crystals, mp 228-230 ^{o}C. UV-Vis (1% Et_3N-CH_2Cl_2): λ_{max} (log ε) 398 (5.36), 491 (4.23), 588 (3.45), 646 nm (4.31). UV-Vis (5% TFA-CH_2Cl_2): λ_{max} (log ε) 406 (5.30), 423 (5.19), 527 (3.86), 543 (3.86), 583 (3.93), 635 nm (3.99). ^{1}H NMR (500 MHz, $CDCl_3$): δ -7.08 (1H, s, 21-H), 1.80-1.84 (6H, 2 overlapping triplets, J = 7.7 Hz, 8,17-CH_2CH_3), 1.85-1.88 (6H, 2 overlapping triplets, J = 7.7 Hz, 12,13-CH_2CH_3), 3.50 (3H, s, 7-Me), 3.54 (3H, s, 18-Me), 3.90 (6H, s, 2 x OMe), 3.96-4.01 (4H, 2 overlapping quartets, 12,13-CH_2CH_3), 4.04-4.09 (4H, 2 overlapping quartets, 8,17-CH_2CH_3), 5.43 (2H, s, 3-CH_2), 9.25 (1H, s, 5-H), 9.58 (1H, s, 20-H), 9.84 (1H, s), 9.86 (1H, s) (10,15-H). ^{13}C NMR (125 MHz, $CDCl_3$): δ 11.4 (7-Me), 11.6 (18-Me), 17.6 (8,17-CH_2CH_3), 18.8 (12,13-CH_2CH_3), 19.8 (8,17-CH_2CH_3), 20.2 (12,13-CH_2CH_3), 45.3 (3-CH_2), 53.5 (2 x OMe, 67.7 (C-2), 96.2 (10- or 15-CH), 96.5 (10- or 15-CH), 97.7 (5-CH), 99.3 (20-CH), 120.7 (21-CH), 129.7, 130.2, 132.95, 133.05, 135.5, 135.8, 137.8, 137.9, 139.8, 140.6, 143.3, 143.4, 150.5, 172.2 (2 x C=O). ^{1}H NMR (500 MHz, 5% TFA-$CDCl_3$): δ -7.10 (1H, s, 21-CH), -5.96 (1H, br s, NH), -4.95 (2H, br s, 2 x NH), 1.67-1.72 (6H, 2 overlapping triplets, 8,17-CH_2CH_3), 1.83-1.87 (2 overlapping triplets, 12,13-CH_2CH_3), 3.49 (3H, s, 7-Me), 3.51 (3H, s, 18-Me), 3.98 (6H, s, 2 x OMe), 4.09 (4H, q, J = 7.7 Hz, 8,17-CH_2), 4.16 (4H, q, J = 7.6 Hz, 12,13-CH_2), 9.71 (1H, s, 5-H), 9.96 (1H, s, 20-H), 10.226 (1H, s), 10.231 (1H, s) (10,15-H). ^{13}C NMR (125 MHz, 5% TFA-$CDCl_3$): δ 11.44, 11.47 (7,18-Me), 16.6 (8,17-CH_2CH_3), 17.6 (12,13-

CH_2CH_3), 20.1 (12,13-CH_2CH_3), 20.2 (8,17-CH_2CH_3), 45.7 (3-CH_2), 55.1 (2 x OMe), 68.4 (2-C), 94.6 (10- or 15-CH), 94.7 (10- or 15-CH), 103.7 (5-CH), 103.9 (20-CH), 128.6 (21-CH), 134.5, 134.8, 134.9, 135.1, 135.6, 135.9, 141.4, 142.0, 142.1, 142.7, 142.9, 143.0, 145.0, 173.7 (2 x C=O). HRMS (ESI): calcd for $C_{35}H_{41}N_3O_4$ + H 568.3175, found 568.3177.

8,12,13,17-Tetraethyl-2,3-dimethoxycarbonyl-7,18-dimethyl-21-carbaporphyrinato)silver(III) (**27a**). A solution of carbaporphyrin **26** (10.0 mg, 0.0177 mmol) in dichloromethane (10 mL) was added to silver(I) acetate (11 mg, 0.066 mmol) in methanol (2.5 mL), and the mixture stirred at room temperature overnight. The mixture was washed with water, and the solvent was removed under reduced pressure. The residue was purified by column chromatography on grade 3 neutral alumina eluting with 60:40 dichloromethane-hexanes. A deep red fraction was collected and recrystallized from chloroform-methanol to give the silver(III) complex (7.2 mg, 0.011 mmol, 61%) as a red powder, mp >300 °C. UV-Vis (CH_2Cl_2): λ_{max} (log ε) 309 (4.06), 352 (4.29), 376 (4.29), 407 (4.44), 449 (4.64), 515 (3.63), 567 nm (4.13). ^{1}H NMR (500 MHz, $CDCl_3$): δ 1.59 (12H, t, J = 7.7 Hz, 4 x CH_2CH_3), 3.31 (6H, s, 7,18-Me), 3.59 (4H, q, J = 7.7 Hz, 12,13-CH_2), 3.64 (4H, q, J = 7.7 Hz, 8,17-CH_2), 4.40 (6H, s, 2 x OMe), 8.79 (2H, s, 10,15-H), 9.90 (2H, s, 5,20-H). ^{13}C NMR (125 MHz, $CDCl_3$): δ 11.5 (7,18-Me), 17.3 (2 x CH_2CH_3), 18.1 (2 x CH_2CH_3), 19.4 (12,13-CH_2), 20.0 (8,17-CH_2), 52.6 (2 x OMe), 96.1 (10,15-CH), 110.1 (5,20-CH), 118.3, 131.1, 134.51 (d, J = 3.3 Hz), 134.57 (d, J = 3.5 Hz), 137.2, 138.3, 139.6 (d, J = 3.2 Hz), 140.9, 167.5 (2 x C=O). HRMS (EI): calcd for $C_{35}H_{36}AgN_3O_4$ 669.1757, found 669.1752.

8,12,13,17-Tetraethyl-2,3-dimethoxycarbonyl-7,18-dimethyl-2,3-dihydro-21-carbaporphyrinato)silver(III) (**38**). Carbachlorin **32** (10.0 mg, 0.0176 mmol) in

dichloromethane (10 mL) was reacted with silver(I) acetate (12 mg, 0.019 mmol) in methanol (2.5 mL) as described above. Purification by column chromatography on neutral grade 3 alumina eluting with 60:40 dichloromethane-hexane gave a deep red fraction and subsequent recrystallization from chloroform-methanol afforded the silver(III) carbachlorin (7.3 mg, 0.011 mmol, 62%) as a red powder, mp 266-268 ^{o}C. UV-Vis (CH_2Cl_2): λ_{max} (log ε) 386 (sh, 4.49), 410 (5.15), 490 (3.96), 522 (3.82), 546 (3.58), 592 nm (4.43). ^{1}H NMR (500 MHz, $CDCl_3$): 1.81 (3H, t, *J* = 7.7 Hz), 1.83 (3H, t, *J* = 7.7 Hz), 1.88 (6H, t, *J* = 7.7 Hz) (4 x CH_2CH_3), 3.47 (3H, s, 7-Me), 3.54 (3H, s, 18-Me), 3.93 (6H, s, 2 x OMe), 3.98-4.09 (8H, m, 4 x CH_2CH_3), 9.36 (1H, s, 5-H), 9.70 (1H, s, 20-H), 9.93 (1H, s), 9.98 (1H, s) (10,15-H). ^{13}C NMR (125 MHz, $CDCl_3$): δ 11.8 (7-Me), 12.0 (18-Me), 17.82, 17.83, 18.58, 18.59, 19.9, 20.48, 20.52, 45.3 (3-CH_2), 53.5 (2 x OMe), 67.5 (C-2), 98.2 (10- or 15-CH), 98.5 (10- or 15-CH), 101.3 (d, *J* = 2.5 Hz, 5-CH), 103.0 (d, *J* = 2.6 Hz, 20-CH), 129.0, 129.6, 130.2 (d, *J* = 3.8 Hz), 130.8 (d, *J* = 3.8 Hz), 133.4, 133.5, 134.2, 134.4, 136.0 (d, *J* = 3.1 Hz), 136.5 (d, *J* = 3.1 Hz), 138.7, 138.8, 140.3 (d, *J* = 2.7 Hz), 140.6 (d, *J* = 3.1 Hz), 172.4 (2 x C=O). HRMS (ESI): calcd for $C_{35}H_{38}AgN_3O_4$ + H 672.1992, found 672.2007.

8,12,13,17-Tetraethyl-2,3-dimethoxycarbonyl-7,18-dimethyl-21-carbaporphyrinato)gold(III) (**27b**). A solution of gold(III) acetate (15 mg, 0.04 mmol) in pyridine (2 mL) was added to a solution of carbaporphyrin **26** (15.0 mg, 0.0265 mmol) in pyridine (13 mL), and the resulting mixture was stirred under reflux for 30 min. The mixture was diluted with chloroform, washed with water and the solvent evaporated under reduced pressure. The residue was purified by column chromatography on grade 3 alumina eluting with 60:40 dichloromethane-hexanes, and the product was collected as a dark red fraction. Recrystallization

from chloroform-methanol gave the gold complex (8.9 mg, 0.0117 mmol, 44%) as a red powder, mp 260-262 ^{o}C. UV-Vis ($CHCl_3$): λ_{max} (log ε) 348 (4.38), 373 (4.35), 403 (4.41), 441 (4.43), 474 (sh, 3.83), 513 (3.76), 557 nm (4.41). ^{1}H NMR (500 MHz, $CDCl_3$): δ 1.63-1.68 (12H, t, J = 7.7 Hz, 4 x CH_2CH_3), 3.36 (6H, s, 7,18-Me), 3.69 (4H, q, J = 7.7 Hz, 12,13-CH_2), 3.74 (4H, q, J = 7.7 Hz, 8,17-CH_2), 4.36 (6H, s, 2 x OMe), 9.02 (2H, s, 10,15-H), 9.99 (2H, s, 5,20-H). ^{13}C NMR (125 MHz, $CDCl_3$): δ 11.5 (7,18-Me), 17.3 (8,17-CH_2CH_3), 18.0 (12,13-CH_2CH_3), 19.4 (12,13-CH_2), 19.8 (8,17-CH_2), 52.5 (2 x OMe), 96.3 (10,15-CH), 111.4 (5,20-CH), 122.1, 134.07, 134.14, 135.1, 136.2, 137.3, 138.2 140.9, 167.5 (2 x C=O). HRMS (ESI): calcd for $C_{35}H_{36}AuN_3O_4$ + H 760.2450, found 760.2460.

8,12,13,17-Tetraethyl-2,3-dimethoxycarbonyl-7,18,21-trimethyl-21-carbaporphyrin (**28**). Carbaporphyrin **26** (12.0 mg, 0.021 mmol) was stirred with potassium carbonate (12 mg) and methyl iodide (6 drops) in acetone (18 mL) under reflux for 30 min. The mixture was suction filtered and the solvent evaporated under reduced pressure. The residue was run through a grade 3 neutral alumina column, eluting with 60:40 dichloromethane-hexanes, and two colored fractions were collected. The later major red fraction was evaporated under reduced pressure and the residue recrystallized from chloroform-methanol to yield the *C*-methylcarbaporphyrin (9.1 mg, 0.016 mmol, 75%) as purple powder, mp 298-300 ^{o}C. UV-Vis (CH_2Cl_2): λ_{max} (log ε) 312 (4.17), 428 (4.67), 537 (sh, 3.64), 580 (3.92), 647 nm (sh, 3.33). UV-Vis (1% Et_3N-CH_2Cl_2): λ_{max} (log ε) 408 (4.64), 431 (sh, 4.61), 468 (sh, 4.45), 576 (sh, 3.73), 649 (3.90), 701 nm (sh, 3.37). UV-Vis (5% DBU-CH_2Cl_2): λ_{max} (log ε) 405 (4.67), 432 (sh, 4.62), 467 (sh, 4.50), 564 (sh, 3.73), 648 (3.97), 700 nm (sh, 3.38). UV-Vis (5 equiv TFA-CH_2Cl_2): λ_{max} (log ε) 316 (4.16), 411 (4.76), 556 (sh, 3.65), 581 (3.75), 629 nm (sh, 3.45). UV-Vis (25% TFA-CH_2Cl_2): λ_{max} (log ε)

320 (3.78), 414 (5.08), 430 (sh, 4.89), 550 (3.46), 606 nm (3.79). UV-Vis (50% TFA-CH_2Cl_2): λ_{max} (log ε) 316 (3.97), 413 (5.11), 432 (4.92), 529 (sh, 3.50), 549 (sh, 3.48), 598 (3.80), 620 nm (3.80). ^{1}H NMR (500 MHz, $CDCl_3$): δ -4.68 (3H, s, 21-Me), -3.19 (2H, v br, 2 x NH), 1.76-1.80 (12H, 2 overlapping triplets, 4 x CH_2CH_3), 3.43 (6H, s, 7,18-Me), 3.71-3.79 (4H, m, 12,13-CH_2), 3.86 (4H, q, J = 7.6 Hz, 8,17-CH_2), 4.02 (6H, s, 2 x OMe), 9.28 (2H, s, 10,15-H), 9.90 (2H, s, 5,20-H). ^{13}C NMR (125 MHz, $CDCl_3$): δ 10.7 (21-Me), 11.5 (7,18-Me), 17.2 (2 x CH_2CH_3), 18.2 (2 x CH_2CH_3), 19.5 (8,17-CH_2), 19.8 (12,13-CH_2), 52.3 (2 x OMe), 94.4 (10,15-H), 101.6, 109.9 (5,20-H), 118.3, 135.0, 135.1, 135.4, 137.8, 139.8, 145.6, 157.2, 167.0. ^{1}H NMR (500 MHz, DBU-$CDCl_3$, upfield and downfield resonances only for anion [**28** – H]$^-$): δ -4.78 (1H, s, 21-H), 9.22 (2H, s), 9.83 (2H, s) (4 x *meso*-H); ^{1}H NMR (500 MHz, 2 equiv. TFA-$CDCl_3$): δ -5.41 (3H, s, 21-H), -1.5 (1H, v br, 23-NH), -1.42 (2H, s, 22,24-NH), 1.69 (6H, t, J = 7.7 Hz, 8,17-CH_2CH_3), 1.80 (6H, t, J = 7.7 Hz, 12,13- CH_2CH_3) 3.31 (6H, s, 7,18-Me), 3.74-3.88 (6H, m), 3.88-3.96 (2H, m), (4 x CH_2CH_3), 3.98 (6H, s, 2 x OMe), 9.49 (2H, s, 10,15-H), 10.03 (2H, s, 5,20-H). ^{13}C NMR (125 MHz, 2 equiv. TFA-$CDCl_3$): δ 11.1 (21-Me), 11.6 (7,18-Me), 16.7 (8,17- CH_2CH_3), 17.3 (12,13- CH_2CH_3), 19.66 (2 x CH_2CH_3), 19.72 (2 x CH_2CH_3), 52.3 (2 x OMe), 95.0 (10,15-CH), 113.4, 115.0 (5,20-CH), 121.8, 135.4, 138.0, 138.8, 139.7, 140.3, 141.3, 142.5, 166.4. ^{1}H NMR (500 MHz, excess TFA-$CDCl_3$): δ -8.67 (1H, q, J = 7.6 Hz, 21-H), -6.55 (3H, d, J = 7.6 Hz, 21-Me), 1.94 (6H, t, J = 7.6 Hz), 1.97 (6H, t, J = 7.7 Hz) (4 x CH_2CH_3), 3.85 (6H, s, 7,18-Me), 4.30-4.41 (8H, m, 4 x CH_2CH_3), 4.66 (6H, s, 2 x OMe), 11.16 (2H, s), 11.80 (2H, s) (4 x *meso*-H). ^{13}C NMR (125 MHz, excess TFA-$CDCl_3$): δ 11.0 (21-Me), 12.0 (7,18-Me), 16.6, 17.7, 20.7, 20.8, 31.9 (21-CH), 55.5 (2 x OMe), 105.5 (10,15-CH), 114.4 (5,20-CH),

143.3, 144.3, 144.7, 145.9, 146.3, 149.2, 149.7, 150.6, 155.3, 166.9 (2 x C=O). HRMS (ESI): calcd for $C_{36}H_{41}N_3O_4$ + H 580.3175, found 580.3153.

8,12,13,17-Tetraethyl-2,3-dimethoxycarbonyl-7,18,21,22-tetramethyl-21-carbaporphyrin (**29**). Carbaporphyrin **26** (12.0 mg, 0.021 mmol) was stirred with potassium carbonate (12 mg) and methyl iodide (10 drops) in acetone (12 mL) under reflux for 16 h. The mixture was diluted with dichloromethane, washed with water and evaporated under reduced pressure. The residue was purified on a grade 3 neutral alumina column, eluting with 60:40 dichloromethane-hexanes, and a brown colored fraction was collected. Recrystallization from chloroform-methanol yielded the dimethylcarbaporphyrin (8.7 mg, 0.015 mmol, 70%) as purple crystals, mp 232-234 ^{o}C. UV-Vis (CH_2Cl_2): λ_{max} (log ε) 316 (4.41), 376 (4.59), 441 (5.89), 545 (3.93), 589 (4.01), 736 nm (3.30). UV-Vis (CH_2Cl_2): λ_{max} (log ε) 320 (4.34), 412 (4.77), 429 (sh, 4.73), 567 (3.85), 607 nm (sh, 3.76). ^{1}H NMR (500 MHz, $CDCl_3$): δ -5.27 (3H, s, 21-Me), -3.91 (3H, s, 22-Me), 1.39 (3H, t, *J* = 7.6 Hz), 1.70 (3H, t, *J* = 7.7 Hz), 1.73-1.78 (6H, 2 overlapping triplets, *J* = 7.6 Hz) (4 x CH_2CH_3), 2.95 (3H, s, 7-Me), 3.32 (3H, s, 18-Me), 3.37-3.43 (2H, m), 3.55-3.66 (3H, m), 3.68-3.76 (3H, m) (4 x CH_2CH_3), 4.02 (3H, s), 4.06 (3H, s) (2 x OMe), 8.90 (1H, s, 15-H), 9.05 (1H, s, 10-H), 9.52 (1H, s), 9.54 (1H, s) (5,20-H). ^{13}C NMR (125 MHz, $CDCl_3$): δ 9.6 (21-Me), 11.4 (18-Me), 11.7 (7-Me), 16.2, 17.1, 18.0, 18.1, 19.3, 19.57, 19.61, 19.8, 31.7 (22-Me), 52.1, 52.3, 93.7 (15-CH), 98.0 (10-CH), 108.9 (20-CH), 109.5, 112.5 (5-CH), 116.4, 123.3, 128.1, 131.2, 132.5, 134.4, 135.7, 136.1, 137.5, 141.8, 144.3, 145.8, 146.4, 150.6, 154.8, 158.2, 166.5, 167.7. ^{1}H NMR (500 MHz, TFA-$CDCl_3$): δ -4.91 (3H, s, 21-Me), -4.18 (1H, br s, NH), -4.02 (1H, br s, NH), -3.54 (3H, s, 22-Me), 1.46 (3H, t, *J* = 7.7 Hz), 1.72 (3H, t, *J* = 7.7 Hz), 1-80-1.85 (6H, 2 overlapping triplets, *J* = 7.7 Hz) (4 x CH_2CH_3), 3.03 (3H, s, 7-Me), 3.37 (3H, s, 18-Me), 3.46-

3.53 (2H, m), 3.82 (2H, q, J = 7.7 Hz), 3.86-3.97 (4H, m) (4 x CH_2CH$_3$), 4.15 (3H, s), 4.19 (3H, s) (2 x OMe), 9.45 (1H, s), 9.46 (1H, s) (10,15-H), 9.86 (1H, s, 20-H), 9.92 (1H, s, 5-H). ^{13}C NMR (125 MHz, 2 μL TFA-CDCl$_3$): δ 10.9 (21-Me), 11.8, 12.2, 15.8, 16.4, 17.17, 17.23, 19.6, 19.7, 19.8, 31.1 (22-Me), 53.0, 53.1, 92.9, 96.3, 113.3, 114.5, 117.4, 123.1, 134.3, 135.5, 136.5, 138.6, 138.9, 139.4, 141.1, 141.88, 141.94, 142.5, 144.6, 145.2, 150.6, 152.6. HRMS (ESI): calcd for $C_{37}H_{43}N_3O_4$ + H 594.3332, found 594.3326.

(8,12,13,17-Tetraethyl-2,3-dimethoxycarbonyl-7,18,21-trimethyl-21-carbaporphyrinato)palladium(II) (**30**). Palladium(II) acetate (10 mg, 0.044 mmol) was added to a solution of 21-methylcarbaporphyrin **28** (10.0 mg, 0.017 mmol) in acetonitrile (10 mL), and the solution was stirred under reflux for 30 min. The solution was cooled, diluted with chloroform, washed with water, and the organic layer separated and then evaporated to dryness. The residue was purified by column chromatography on grade 3 neutral alumina eluting with 30% dichloromethane-hexanes, and the product collected as a green band. The solvent was evaporated and the residue recrystallized from chloroform-methanol to yield the palladium(II) complex (7.4 mg, 0.011 mmol, 63%) as dark green crystals, mp 286-288 ^{o}C. UV-Vis (CHCl$_3$): λ_{max} (log ε) 306 (4.37), 410 (4.54), 460 (4.52), 602 (3.90), 639 nm (sh, 3.81). ^{1}H NMR (500 MHz, CDCl$_3$): δ -4.12 (3H, s, 21-Me), 1.81 (6H, t, J = 7.7 Hz), 1.83 (6H, t, J = 7.7 Hz) (4 x CH$_2$CH_3), 3.44 (6H, s, 7,18-Me), 3.86-3.92 (8H, 2 overlapping quartets, 4 x CH_2CH$_3$), 4.30 (6H, s, 2 x OMe), 9.85 (2H, s, 10,15-H), 10.81 (2H, s, 5,20-H). ^{13}C NMR (125 MHz, CDCl$_3$): δ 11.9 (7,18-Me), 17.6, 18.4, 19.8, 20.1, 21.8 (21-Me), 36.4 (C-21), 52.9 (2 x OMe), 101.7 (10,15-CH), 113.0 (5,20-CH), 131.3, 136.9, 143.4, 143.9, 145.5, 145.6, 149.2, 158.6, 167.6 (2 x C=O). HRMS (ESI): calcd for $C_{36}H_{39}N_3O_4Pd$ 683.1975, found 683.1955.

(8,12,13,17-Tetraethyl-2,3-dimethoxycarbonyl-7,18,21-trimethyl-21-carbaporphyrinato)nickel(II) (**31**). Nickel(II) acetate tetrahydrate (10 mg, 0.057 mmol) was added to a solution of 21-methylcarbaporphyrin **28** (10.0 mg, 0.017 mmol) in DMF (10 mL), and the solution stirred under reflux for 30 min. The solution was cooled, diluted with chloroform, washed with water, and the organic layer evaporated to dryness. The residue was run through a grade 3 neutral alumina column, eluting with 60% dichloromethane-hexanes, and the product collected as a green band. Recrystallization from chloroform-methanol yielded the nickel(II) complex (7.6 mg, 0.012 mmol, 70%) as dark green crystals, mp 267-269 ^{o}C. UV-Vis ($CHCl_3$): λ_{max} (log ε) 348 (4.51), 420 (4.72), 456 (sh, 4.38), 612 nm (3.96). ^{1}H NMR (500 MHz, $CDCl_3$): δ -3.89 (3H, s, 21-Me), 1.72 (6H, t, *J* = 7.7 Hz, 12,13-CH_2CH_3), 1.77 (6H, t, *J* = 7.7 Hz, 8,17-CH_2CH_3), 3.31 (6H, s, 7,18-Me), 3.72-3.81 (8H, m, 4 x CH_2CH_3), 4.26 (6H, s, 2 x OMe), 9.59 (2H, s, 10,15-H), 10.56 (2H, s, 5,20-H). ^{13}C NMR (125 MHz, $CDCl_3$): δ 11.8 (7,18-Me), 17.5 (12,13-CH_2CH_3), 18.2 (8,17-CH_2CH_3), 19.7 (2 x CH_2CH_3), 19.8 (21-Me), 19.9 (2 x CH_2CH_3), 26.7 (C-21), 52.8 (2 x OMe), 99.8 (10,15-CH), 111.0 (5,20-CH), 131.3, 138.3, 144.3, 145.9, 146.1, 148.7, 150.9, 167.6 (2 x C=O). HRMS (ESI): calcd for $C_{36}H_{39}N_3O_4Ni$ 635.2294, found 635.2285.

ASSOCIATED CONTENT

Supplementary Information

The Supporting Information is available free of charge on the ACS Publications website.

Crystallographic experimental details, cif files for compounds **26**, **30**, **31** and **32**, and selected ^{1}H NMR, ^{1}H-^{1}H COSY, HMQC, ^{13}C NMR, DEPT-135, MS, and UV-Vis spectra (PDF).

AUTHOR INFORMATION

Corresponding Author

* E-mail: tdlash@ilstu.edu

ORCID

Timothy D. Lash: 0000-0002-0050-0385

Notes

The authors declare no competing financial interest.

ACKNOWLEDGMENTS

This work was supported by the National Science Foundation under grants CHE-1212691 and CHE-1465049, and the Petroleum Research Fund, administered by the American Chemical Society. The authors thank Dr. Mathias Zeller for useful discussion regarding optimal refinement of the crystallographic data for compound **32**, and thank NSF-CHE (grant #1039689) for funding the X-ray diffractometer.

REFERENCES

1. (a) Lindsey, J. S. *Chem. Rev.* **2015**, *115*, 6534-6620. (b) Taniguchi, M.; Lindsey, J. S. *Chem. Rev.* **2017**, *117*, 344-535.
2. Scheer, H. In *Chlorophylls*; Scheer, H, Ed.; CRC Press: Boca Raton, FL, 1991; pp 3-30.
3. (a) Timkovich, R.; Cork, M. S.; Gennis, R. B.; Johnson, P. Y. *J. Am. Chem. Soc.* **1985**, *107*, 6069-6075. (b) Murshudov, G. N.; Grebenko, A. I.; Barynin, V.; Dauter, Z.; Wilson, K. S.;

Vainshtein, B. K.; Melik-Adamyan, W.; Bravo, J.; Ferran, J. M.; Ferrer, J. C.; Switala, J.; Loewen, P. C.; Fita, I. *J. Biol. Chem.* **1996**, *271*, 8863-8868.

4. (a) Pelter, A.; Ballantine, J. A.; Ferrito, V.; Jaccarini, V.; Psaila, A.; Schembri, P. J. *J. Chem. Soc., Chem. Commun.* **1976**, 999-1000. (b) Dutton, C. J.; Fookes, C. J. R.; Battersby, A. R. *J. Chem. Soc., Chem. Commun.* **1983**, 1237-1238. (c) Montforts, F.-P.; Schwartz, U. M. *Angew. Chem. Int. Ed. Engl.* **1985**, *24*, 775-776.

5. (a) Karuso, P.; Berquist, P. R.; Buckleton, J. S.; Cambie, R. C.; Clark, G. R.; Richard, C. E. F. *Tetrahedron Lett.***1986**, *27*, 2177-2178. (b) Schopf, J. W. In *Earth's Earliest Biosphere: Its Origin and Evolution*; Schopf, J. W., Ed.; Princeton University Press: Princeton, 1983; p 543. (c) Bible, K. C.; Buyendorp, M.; Zierath, P. D.; Rinehart, K. L. *Proc. Natl. Acad. Sci.* **1988**, *85*, 4582-4586. (d) Sakata, K.; Yamamoto, K.; Ishikawa, H.; Yagi, A.; Etoh, H.; Ina, K. *Tetrahedron Lett.* **1990**, *31*, 1165-1168. (e) Yamamoto, K.; Sakata, K.; Watanabe, N.; Yagi, A.; Brinen, L. S.; Clardy, J. *Tetrahedron Lett.* **1992**, *33*, 2587-2588. (f) Watanabe N., Yamamoto K., Ishikawa H., Yagi A., Sakata K., Brinen L. S., and Clardy J. *J. Nat. Prod.* **1993**, *56***,** 305–317. (g) Dolphin, D.; Ma, L. *J. Org. Chem.* **1996**, *61*, 2501-2510.

6. (a) Scott, L. J.; Goa, K. L. *Drugs & Aging* **2000**, *16*, 139-146. (b) Karim, S. P.; Adelman, R. A. *Clin. Ophthalmol.* **2013**, *7*, 1867-1875. (c) Ethirajan, M.; Chen, Y.; Joshi, P.; Pandey, R. K. *Chem. Soc. Rev.* **2011**, *40*, 340-362.

7. Jain, M.; Zellweger, M.; Frobert, A.; Valentin, J.; van den Bergh, H.; Wagnieres, G.; Cook, S.; Giraud, M.-N. *Front. Physiol.* **2016**, *7*, 400.

8. Senge, M. O.; Brandt, J. C. *Photochem. Photobiol.* **2011**, *87*, 1240-1296. (b) Senge, M. O. *Photodiagnosis Photodyn. Ther.* **2012**, *9*, 170-179. (c) de Visscher, S. A.; Dijkstra, P. U.; Tan, I. B.; Roodenburg, J. L.; Witjes, M. *J. Oral Oncol.* **2013**, *49*, 192-210.

9. (a) Wang, S.; Bromley, E.; Xu, L.; Chen, J. C.; Keltner, L. *Expert Opin. Pharmocother.* **2010**, *11*, 133-140. (b) Miki, Y.; Akimoto, J.; Hiranuma, M.; Fujiwara, Y. *J. Toxicol. Sci.* **2014**, *39*, 821-827.

10. (a) MacDonald, I. J.; Dougherty, T. J. *J. Porphyrins Phthalocyanines* **2001**, *5*, 105-129. (b) Bonnett, R. *Chem. Soc. Rev.* **1995**, *24*, 19-33.

11. Pandey, R. K.; Zheng, G. In *The Porphyrin Handbook*, Kadish, K. M., Smith, K. M., Guilard, R., Eds.; Academic Press: San Diego, CA, 2000; Vol. 6, pp 157−230.

12. (a) Callot, H. J.; Schaeffer, E. *Tetrahedron* **1978**, *34*, 2295−2300. (b) Vogel, E.; Kocher, M.; Balchi, M.; Teichler, I.; Lex, J.; Schmickler, H.; Ermer, O. *Angew. Chem., Int. Ed. Engl.* **1987**, *36*, 931-934. (c) McCarthy, J. R.; Jenkins, H. A.; Brückner, C. *Org. Lett.* **2003**, *5*, 19−22. (d) Lara, K. K.; Rinaldo, C. R.; Bruckner, C. *Tetrahedron Lett.* **2003**, *44*, 7793-7796. (e) Akhigbe, J.; Haskoor, J.; Krause, J. A.; Zeller, M.; Brückner, C. *Org. Biomol. Chem.* **2013**, *11*, 3616-3628. (f) Ogikubo, J.; Meehan, E.; Engle, J. T.; Ziegler, C. J.; Brückner, C. *J. Org. Chem.* **2012**, *77*, 6199-6207. (g) Li, R.; Meehan, E.; Zeller, M.; Brückner, C. *Eur. J. Org. Chem.* **2017**, 1826-1834.

13. Lash, T. D. *Chem. Rev.* **2017**, *117*, 2313-2446.

14. (a) Toganoh, M.; Furuta, H. In *Handbook of Porphyrin Science – With Applications to Chemistry, Physics, Material Science, Engineering, Biology and Medicine*, Vol. 2, Kadish,

K. M.; Smith, K. M.; Guilard, R., eds.; World Scientific Publishing: Singapore, 2010, pp 295-367. (b) Toganoh, M.; Furuta, H. *Chem. Commun.* **2012**, *48*, 937-954.

15. Lash, T. D. *Acc. Chem. Res.* **2016**, *49*, 471-482.
16. Lash, T. D. *Org. Biomol. Chem.* **2015**, *13*, 7846-7878.
17. Stepien, M.; Latos-Grazyński, L.; Szterenberg, L.; Panek, J.; Latajka, Z. *J. Am. Chem. Soc.* **2004**, *126*, 4566-4580.
18. Stepien, M.; Latos-Grazyński, L. *Acc. Chem. Res.* **2005**, *38*, 88-98.
19. (a) Lash, T. D.; Pokharel, K.; Zeller, M.; Ferrence, G. M. *Chem. Commun.* **2012**, *48*, 11793-11795. (b) Stateman, L. M.; Ferrence, G. M.; Lash, T. D. *Organometallics* **2015**, *34*, 3842-3848.
20. (a) Lash, T. D.; Hayes, M. J. *Angew. Chem. Int. Ed. Engl.* **1997**, *36*, 840-842. (b) Lash, T. D.; Hayes, M. J.; Spence, J. D.; Muckey, M. A.; Ferrence, G. M.; Szczepura, L. F. *J. Org. Chem.* **2002**, *67*, 4860-4874.
21. Li, D.; Lash, T. D. *J. Org. Chem.* **2014**, *79*, 7112-7121.
22. Lash, T. D. *J. Porphyrins Phthalocyanines* **2016**, *20*, 855-888.
23. (a) Muckey, M. A.; Szczepura, L. F.; Ferrence, G. M.; Lash, T. D. *Inorg. Chem.* **2002**, *41*, 4840-4842. (b) Lash, T. D.; Colby, D. A.; Szczepura, L. F. *Inorg. Chem.* **2004**, *43*, 5258-5267.
24. Adiraju, V. A. K.; Ferrence, G. M.; Lash, T. D. *Dalton Trans.* **2016**, *45*, 13691-13694.
25. Lash, T. D. *Org. Lett.* **2011**, *13*, 4632-4635.
26. Szyszko, B.; Latos-Grazyński, L.; Szterenberg, L. *Angew. Chem., Int. Ed.* **2011**, *50*, 6587-6591.

27. (a) Szyszko, B.; Kupietz,K.; Szterenberg, L.; Latos-Grazyński, L. *Chem. Eur. J.* **2014**, *20*, 1376-1382. (b) Hurej, K.; Pawlicki, M.; Latos-Grazyński, L. *Chem. Eur. J.* **2017**, *23*, 2059-2066.

28. (a) Idec, A.; Szterenberg, L.; Latos-Grazyński, L. *Chem. Eur. J.* **2015**, *21*, 12481-12487. (b) Hurej, K.; Pawlicki, M.; Szterenberg, L.; Latos-Grazyński, L. *Angew. Chem., Int. Ed.* **2016**, *55*, 1427-1431.

29. Hayes, M. J.; Lash, T. D. *Chem. Eur. J.* **1998**, *4*, 508-511.

30. Lash, T. D.; AbuSalim, D. I.; Ferrence, G. M. *Chem. Commun.* **2015**, *51*, 15952-15955.

31. Berlicka, A.; Dutka, P.; Szterenberg, L.; Latos-Grazyński, L. *Angew. Chem., Int. Ed.* **2014**, *53*, 4885-4889.

32. Results presented in part at the *253rd ACS National Meeting*, San Francisco, CA, April 2-6, 2017. Abstract: Sahota, N.; Lash, T. D. *Abstracts of Papers*, ORGN-752.

33. Berlicka, A.; Białek, M. J.; Latos-Grazyński, L. *Angew. Chem. Int. Ed.* **2016**, *55*, 11231-11236.

34. For convenience, the structures of **21**, **22**, **23**, **24**, **32**, **33**, **34**, **35** and **38** were rendered as single enantiomers and these are intended to show the relative stereochemistry. However, these compounds were, of course, isolated in racemic form.

35. Beare, K. D.; Yuen, A. K. L.; Masters, A. F.; Maschmeyer, T.; McErlean, S. P. *Chem. Commun.* **2013**, *49*, 8347-8349.

36. Göksu, S.; Altundas, R.; Sutbeyaz, Y. *Synth. Commun.* **2000**, *30*, 1615-1621.

37. Donohoe, T. J.; Jahanshahi, A.; Tucker, M. J.; Bhatti, F. L.; Roslan, I. A.; Kabeshov, M.; Wrigley, G. *Chem. Commun.* **2011**, *47*, 5849-5851.

38. Bruno, I. J.; Cole, J. C.; Kessler, M.; Luo, J.; Motherwell, W. D. S.; Purkis, L. H.; Smith, B. R.; Taylor, R.; Cooper, R. I.; Harris, S. E.; Orpen, A. G. *J. Chem. Inf. Comput. Sci.* **2004**, *44*, 2133-2144.

39. Furuta, H.; Ogawa, T.; Uwatoko, Y.; Araki, K. *Inorg. Chem.* **1999**, *38*, 2676-2682.

40. Chmielewski, P. J.; Latos-Grazyński, L.; Glowiak, T. *J. Am. Chem. Soc,* **1996**, *118*, 5690-5701.

41. Hao, F.; Jiang, H.-W.; Zong, G.; Zhou, Z.; Du, R.-B.; Chen, Q.-Y.; Xiao, J.-C. *J. Org. Chem.* **2012**, *77*, 3604-3608.

42. (a) Hirado, M.; Asaba, K. N.; Kogure, N.; Kitajima, M.; Takayama, H. *Org. Lett.* **2012**, *14*, 5800-5803. (b) Choi, J.; Park, H.; Yoo, H. J.; Kim, S.; Sorensen, E. J.; Lee, C. *J. Am. Chem. Soc.* **2014**, *136*, 9918-9921.

43 Nelson, W. L.; Freeman, D. S. Sankar, R. *J. Org. Chem.* **1975**, *40*, 3658-3664.

44. Ponticello, I. S. *J. Polymer Sci., Polymer Chem. Ed.* **1979**, *17*, 3509-3518.

45. Henderson, L. C.; Li, J.; Nation, R. L.; Velkov, T.; Pfeffer, F. M. *Chem. Commun.* **2010**, *46*, 3197-3199.

46. Hickey, S. M.; Ashton, T. D.; White, J. M.; Li, J.; Nation, R. L.; Yu, H. Y.; Elliott, A. G.; Butler, M. S.; Huang, M. S.; Cooper, M. A.; Pfeffer, F. M. *RSC Adv.* **2015**, *5*, 28582-28596.